Semi-annual Technical Report
for the Period 7/1/70-12/31/70

Conduction Mechanisms in Thick Film Microcircuits

Grant Number: DAHC15-70-G7

ARPA Order No.: 1642

Grantee: Purdue Research Foundation

Principal Investigator: R. W. Vest
(317) 494-4445

Effective Date of Grant: 7/1/70

Grant Expiration Date: 6/30/73

Amount of Grant: $49,500

February 1, 1971

Forward

The research described in this report constitutes the first six months effort under a grant from the Advanced Research Projects Agnency, Department of Defense under the technical cognizance of Dr. Norman Tallan, Aerospace Research Laboratories, United States Air Force. The research was conducted in the Turner Laboratory for Electroceramics, School of Electrical Engineering and School of Materials Science and Metallurgical Engineering, Purdue University, Lafayette, Indiana 47907, under the direction of Professor R. W. Vest. Contributing to the project were Mr. G. L. Fuller, Mr. D. J. Deputy, and Mr. J. L. Wright.

Abstract

Previous work on conduction mechanisms in thick film microcircuits is reviewed and the goals of the current project outlined. The design and performance of a programmable time-temperature firing facility, and an automatic resistance measuring system is described. The test system chosen for thick film resistor studies was ruthenium dioxide conductive, $PbO-B_2O_3-SiO_2$ glass, and 96% Al_2O_3 substrate. Published data on the thermophysical properties of each of these ingredients are discussed, and results from this project are included to more nearly complete the characterization of each. The contact resistance of RuO_2 powder was measured as a function of isostatic pressure; a change by only a factor of two was observed up to 15,000 psi. Studies of small RuO_2 single crystals encased in glass indicated a very low solubility. The resistance of an RuO_2 resistor during fabrication was measured, and the results are compared to the behavior of the RuO_2 single crystals in glass.

Table of Contents

List of Figures

List of Tables

I. Introduction

A. Thick Film Technology

Many of the needs for lightweight and compact electronic devices that are beyond the range of monolithic integrated circuit technology can be satisfied by combining monolithic and thick film technologies. Design functions such as flexibility in component use, tight electrical tolerances, high voltage requirements, and power dissipation that are difficult in monolithic design can be obtained in these "hybrid" devices while still maintaining the high degree of stability and reliability required for computer and military applications.

Thick film components are produced by screen printing with compositions (called formulations, inks, or paints) through masks onto a ceramic substrate. These formulations are mixtures of organic screening agents, glass powder (frit), an active ingredient (conductive, resistive, or insulating material), and additives which influence specific areas of performance. After screening, the film is fired at a high temperature to remove the organics and to develop the proper microstructure among the inorganic ingredients. The resulting film is typically 0.5 to 2 mils (12 to 50 μm) thick.

B. Conduction Mechanisms

The current status of thick film technology as applied to conductive and resistive formulations is largely the result of empirical developments. The development of new materials as well as the improvement of existing systems have been hindered by an inadequate understanding of the mechanisms by which electric charge is transported in thick film resistors and conductors.

Any model for conduction in thick film microcircuits must explain results such as those shown in Fig. 1. A correction has been made for the volume fraction

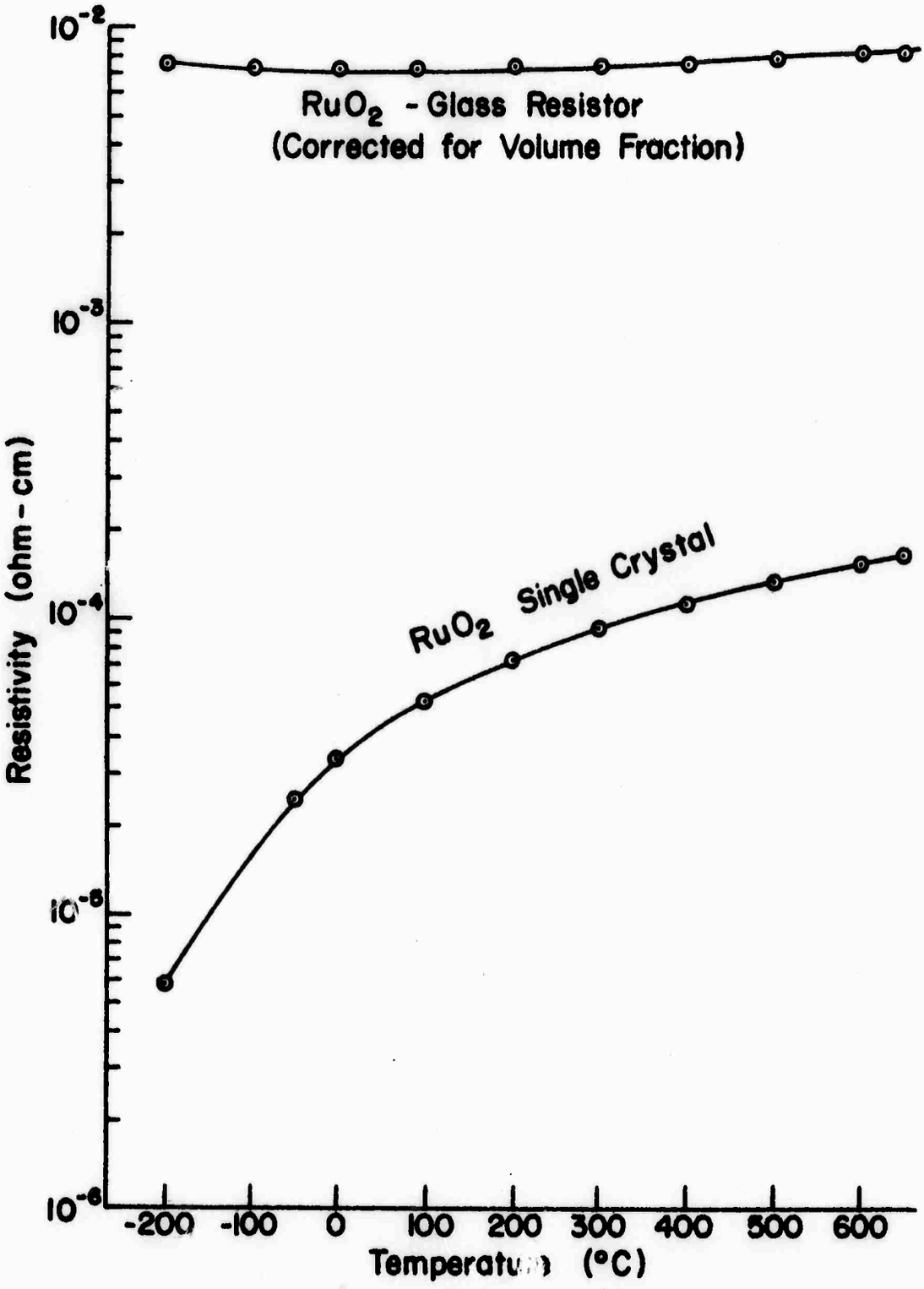

Figure 1. Resistivity of Single Crystal RuO_2 and RuO_2 Resistor Showing the "TCR Anomaly"

of ruthenium dioxide in the resistor; therefore, the data represent the apparent resistivity of RuO_2 in the film. The temperature dependence of the resistivity of single crystal ruthenium dioxide will be further discussed in Section IIIA4 of this report, but it is obvious that the plotted resistivities differ considerably in both magnitude and temperature dependence. This phenomena is not unique to an RuO_2-glass composite, but rather is common to all resistor systems which have been studied.

It would be expected that in a resistor containing many small particles there would be regions of RuO_2 electrically isolated by the glass binder. Also, continuous filaments of RuO_2 between the resistor terminations would result in an additional geometry factor which would further increase the apparent resistivity. Thus, the difference in magnitudes shown in Fig. 1 can be explained with a straightforward microstructural model.

The difference in temperature coefficient of resistivity (TCR) between the single crystal and resistor is considerably more difficult to incorporate into a consistent model. Several possible approaches to explaining this "TCR Anomaly" are:

1. Changes in contact resistance between adjacent particles due to thermal stresses
2. Changes in the intrinsic properties of the conductive material during processing
3. Formation of new phases which contribute to the conduction
4. Size effects which change the intrinsic properties of the conductive
5. Changes in the geometry factor with temperature

There are several ways by which thermal stresses can influence the electrical resistivity of thick film microcircuits. For any isotropic material the measured temperature coefficient of resistance (TCR) is related to the intrinsic temperature coefficient of resistivity (TCρ) by:

$$\frac{1}{R}\frac{dR}{dT} = \frac{1}{\rho}\frac{d\rho}{dT} - \frac{1}{\ell}\frac{d\ell}{dT}$$

$$TCR = TC\rho - \alpha_{\ell} \qquad (1)$$

where α_{ℓ} is the linear coefficient of thermal expansion. If the material is deposited as a film on a substrate which has a different linear coefficient of thermal expansion, Eq. (1) is modified [1] to:

$$TCR = TC\rho - \alpha_{\ell f} - \frac{2(\alpha_{\ell f}-\alpha_{\ell s})}{(1-\mu_f)}\left[\gamma(1-\mu_f)+\mu_f(1-\gamma)\right] \qquad (2)$$

where μ_f = Poisson's ratio of the film material

$\alpha_{\ell f}$ = linear coefficient of thermal expansion of the film material

$\alpha_{\ell s}$ = linear coefficient of thermal expansion of the substrate material

γ = strain coefficient of resistivity = $\frac{1}{\rho}\frac{\partial \rho}{\partial \epsilon}$

ϵ = thermal strain in the plane of the film

The advantage of Eq. (2) is that if the resistor material can be processed into a self-supporting shape, such as a cylinder, so that the necessary parameters can be measured, then it should be possible to predict the TCR of the film resistor on any substrate material. The only restriction of this method is that the substrate completely control the expansion of the film. This is not unreasonable for typical thick film conditions.

Thermal stresses can also be significant when the concept of particle-to-particle contact resistance is introduced. The idea is basically as follows: Thick film resistors are made with glass and conductive particles. Since the glass is an insulator and the resistor conducts, the particles must be in contact with each other. If the contact resistance is significant then any pressure forcing the particles together should be important. For example, in RuO_2 resistors the large positive TCR of the RuO_2 could be offset by a changing contact resistance. As the temperature increases, increasing the resistance of the RuO_2, the differences in thermal coefficients of expansion could cause

the particles of RuO_2 to be pushed together more tightly, decreasing the contact resistance. If the expansion coefficients are chosen correctly it should be possible to have a nearly zero TCR.

This pressure dependent partical contact resistance concept has been pursued by Brady [2] who assumed that the conductance of the resistor was due to a network of conductors in the form of overlapping cylinder or needle shaped elements arranged in a "jack-straw" fashion. The approach then concentrates on the resistance that might be formed at the interface between two contacting cylinders, although the derivation is equally valid for spherical particles. The change in this constriction resistance with pressure (temperature) must be a significant factor in the observed resistor TCR. This basic approach has been applied [3] to correlate data obtained from resistors made with iridium dioxide powder and glass. The resistors were both thick film resistors prepared on a substrate and parallelopiped sintered samples measuring 80mm x 20mm x 10mm. It was believed that the pellets were identical in structure and composition to the thick film resistors. The monotonic relationship observed between the TCR and the differences in linear coefficients of thermal expansion of the different materials was interpreted utilizing the particle contact resistance concept. A transmission electron micrograph of what was felt to be a typical thick film resistor showed clusters of particles ($\sim 1\ \mu m$) forming a semicontinuous network with some evidence of dissolved material close to the particles. This micrograph was used as additional evidence to support the hypothesis of contacting particles.

The particle-to-particle contact resistance concept has been criticized by Collins [4] who proposed that structural models of resistive glazes based on a distribution of physically discrete conductor particles within a glass cannot account for the most important characteristics of real composite resistive systems (such as resistance range, TCR, linearity, noise, etc.) due

to the unstable nature of the contact resistance between individual particles. To support this premise, several examples of unstable or nonohmic conductive particle systems are given. These include:

1. Resistors made with discrete particles usually have a high noise level, higher than typical thick film resistors
2. The resistance of compacted powders can be very pressure dependent and this should cause lack of repeatability in resistor formation
3. Thick film resistors prepared with carbonyl iron powder and copper powder have a non-linear resistance
4. If a thin insulating layer is formed between the particles the resistance would be highly dependent on field strength and temperature

Additional evidence is that substrates with RuO_2 thick film resistors can be subjected to bending stresses to the point of breakage, with the resistor in tension or compression, and the resistance change is never greater than 1%; Collins feels this would not be possible in a system dependent on particle contact resistances.

An alternate microstructure was proposed by Collins [4] consisting of continuous conductive paths meandering through the glass matrix. In this case the resistor would have the properties of the material in the conductive path, but no suggestions were offered as to nature of this material. Presumably the properties of the conductive path would depend on both changes in the intrinsic properties of the conductive during processing and the formation of new phases which contribute to the conduction (Items 2 and 3 given previously). This model is similar to that proposed for palladium-silver resistors [5,6] which requires a microstructure of PdO surrounded by Pd-Ag solid solution with the negative TCR of the semiconducting PdO compensating for the positive TCR of the metal phase. Additions of Nb_2O_5 to thick film formulations with a conductive consisting of RuO_2 are reported [7] to cause large changes in resistor parameters.

For example, in one case a reduction in TCR by a factor of ten was accomplished with a niobium content of 5 atomic percent. It was proposed that the change in the intrinsic properties of the conductive during processing was due to the fact (assumed) that RuO_2 is usually defective in oxygen, probably with a corresponding amount of Ru^{3+} in place of the Ru^{4+} in the crystal lattice. These deviating vacancies were proposed as the cause of variations in resistor performance, and addition of a pentavalent oxide, Nb_2O_5, was the method chosen to balance the vacancies. It was also proposed that since the TCR of ruthenium dioxide is very positive, the addition of a compensating oxide might be expected to lower the TCR and thereby be a TCR control for the resistors.

The formation of new phases which contribute to the conduction is the basis of a model proposed by Sartain [8]. His argument is based on the observation that curves of the resistance vs. temperature of thick film resistors made with IrO_2 or RuO_2, and the resistance vs. temperature of a glass are similar to the corresponding curves of heavily doped and intrinsic silicon. The resistivity of the glass is similar to that of the intrinsic silicon and the resistivity of the doped silicon is similar to the glass with IrO_2 added. The conclusion is that IrO_2 or RuO_2 has produced a semiconducting glass that is degenerate at high levels of doping.

The resistivity of the RuO_2 resistors was found [8] to be dependent on the oxygen partial pressure. With the assumption that this is a linear dependence, it was concluded that the number of holes (the Seebeck coefficient indicates hole conduction) is proportional to the number of oxygen atoms associated with ruthenium. The observed increase in conductivity with increased peak firing temperature is proposed to be due to more ruthenium being oxidized to RuO_2, thus, contributing more holes. Much of the ruthenium not in the form of RuO_2 is supposedly in the form of Ru_2O_3 which acts as an insulator in the glass.

There are no known studies of the variation of intrinsic properties of thick film conductives with particle size, but results showing the effect of RuO_2 particle sizes and shapes on resistor TCR have been reported [9]. It was observed that the TCR tended to increase with increasing particle size of RuO_2, but no quantitative conclusions could be drawn.

In summary, none of the conduction mechanism models which have been proposed will correlate all of the observed results, several of the models contradict one another, and not all posibilities were mentioned. For example, one possible microstructure would be continuous paths of polycrystalline conductive formed by reactive sintering of the particles. Such a structure could be expected to have a large number of impurities in the conductive grain boundaries from the glass. This would introduce temperature independent electron scattering that could account for much of the decrease in TCR, although it probably would not account for negative TCR's reported for high resistivities.

C. Project Goals and Plans

The primary problem in reaching an understanding of typical industrially processed thick film resistor and conductor systems is the complexity of the total manufacturing operation. The large number of variables which influence the value of the resistor make it extremely difficult to purposely change one variable and be certain that some other variable is not changing unexpectedly and completely distorting the meaning of the experimental data. In particular, many resistor systems have small amounts of ingredients added because experience has shown that they improve TCR, stability, etc. From the standpoint of scientific understanding, however, they only cause confusion.

It is felt that the only way to reach an understanding of thick film resistors and conductors is to first perform experiments with the basic ingredient materials and to limit the vareity of experimental samples to those that are as conceptually simple and easy to define as possible. This has been the procedure followed in the initial phase of this project in an

attempt to identify the important material properties and processing variables, and to determine their influence individually on system performance.

The primary thrust of the experimental program is to relate the electrical properties of the thick films to the material properties and processing conditions through microstructure. The materials properties to be correlated are: resistivity; temperature coefficient of resistivity; coefficient of thermal expansion; interfacial energy; particle shape, size, and size distribution; and chemical reactivity with other constituents. The processing conditions to be correlated are time, temperature, and atmosphere during firing. The morphological studies of the fired films will involve the identification of the conducting phases, their size, shape, distribution, composition, and interaction. The thick film resistor portion of this project will use ruthenium dioxide conductive, $PbO-B_2O_3-SiO_2$ glass, and 96% Al_2O_3 substrate as the basis test system to relate material properties to microstructure and system performance. The investigation of thick film conductives involves the study of the noble metals gold, silver, platinum, and palladium, as well as alloys among them.

Based on the experimental results, suitable theories of the electrical properties of heterogeneous systems will be envoked to correlate the data and to aid in the development of phenomological models to inter-relate the various material properties with system performance.

II. Experimental

A. Firing Facility

The most common method of processing thick film resistors and conductors is to use a tunnel kiln. For research and development activities many kiln manufacturers make smaller, somewhat more versatile versions of the larger production equipment. An alternative for research and development is to use ovens; in this case the parts are processed by transferring from oven to oven or varying the temperature of one oven. For many research applications kilns have the disadvantages of limitations in profile versatility, and long times to reach equilibrium if the profile is changed. Processing by varying the temperature of an oven has an even greater limitation in time-temperature versatility. Transferring from oven to oven lacks repeatability and does not closely simulate a tunnel kiln firing.

To overcome these shortcomings, a furnace system has been designed and constructed that can duplicate the profile of any tunnel kiln (within its maximum temperature limit), while allowing rapid changes in profile. The basic system shown in Fig. 2 consists of a tube furnace with a nearly linear temperature profile varying from approximately room temperature at one end to about 1200°C near the center. A sample to be heated is moved back and forth in the tube furance by a servo driven push rod controlled by a program cam wheel. Provision is made to record both temperature and resistance during the firing cycle.

The tube furnace is a three zone, multiple-tap furnace with independent temperature control for all three zones. The center zone is 8.5 cm long, wound with Pt-Rh wires, and is capable of 1500°C. The other two zones are 30 cm long and are wound with Kanthal A-1 alloy. One of the Kanthal zones is part of the linear profile while the other is used for preheating any flowing gas. The

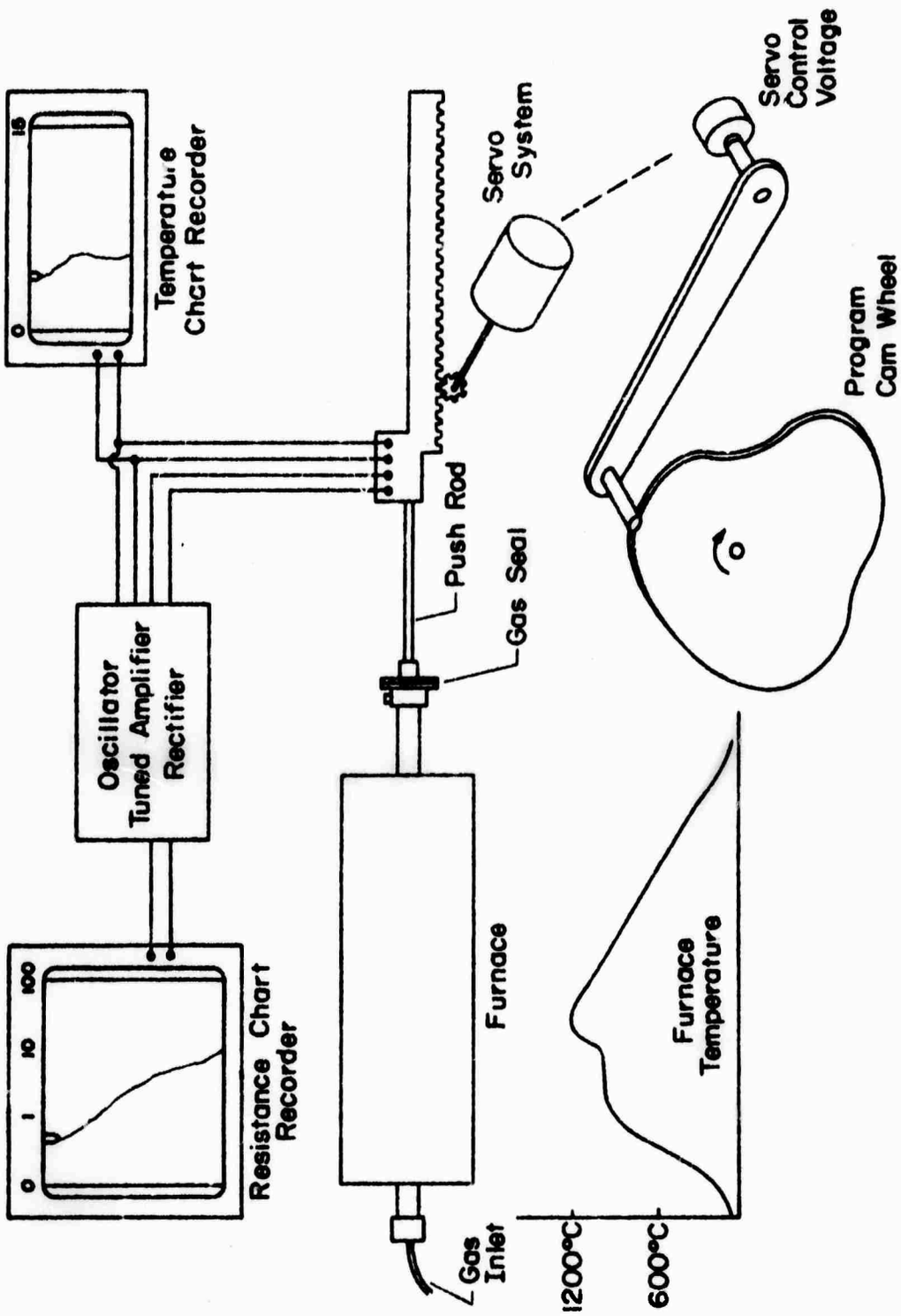

Figure 2. DIAGRAM OF FURNACE AND RESISTANCE MEASURING SYSTEM

furnace tube (2.5 cm I.D.) has gas seals at both ends so that a wide range of atmospheres may be introduced into the furnace.

The part to be fired is placed on an alumina Dee tube that is fastened to a four hole alumina push rod as shown in Fig. 3. Outside the furnace, the other end of the push rod is clamped to a gear rack. The pinion gear is driven by a servomechanism shown schematically in Fig. 4. The shaft for the drive pinion is connected to a ten turn potentiometer which furnishes a feedback voltage proportional to the position of the Dee tube in the furnace. This voltage, minus an input voltage, is the error voltage to the servo amplifier.

The input voltage is usually furnished by either a manually adjusted ten turn potentiometer or by a single turn potentiometer rotated by a lever following the shape of a program cam wheel. An increasing radius of the cam increases the input voltage and causes the sample to be moved to a region of higher temperature. Because the time-temperature relationship is determined by a cam wheel the only delay in changing profiles is the time required to change program cam wheels. The versatility of the time-temperature relationships obtainable with the furnace is limited only by the angular speed of the cam wheel, the maximum speed of motion of the sample in the furnace, and the rate at which the sample can change temperature. Cam wheels are made with the aid of a computer program which takes into account the temperature vs. distance of the furance and the geometry of the cam shaft and lever. The input to the program is the desired temperature versus time and the output is angle-radius points that determine the shape of the cam.

The program cam wheel is rotated by a stepping motor driven by a square wave voltage; the angular rate of rotation is determined by the frequency of this voltage. A block diagram of the cam drive system is shown in Fig. 5. The maximum rate of rotation is one revolution in two minutes and corresponds to 60 Hz. An electronic drive circuit provides 12 additional lower frequency

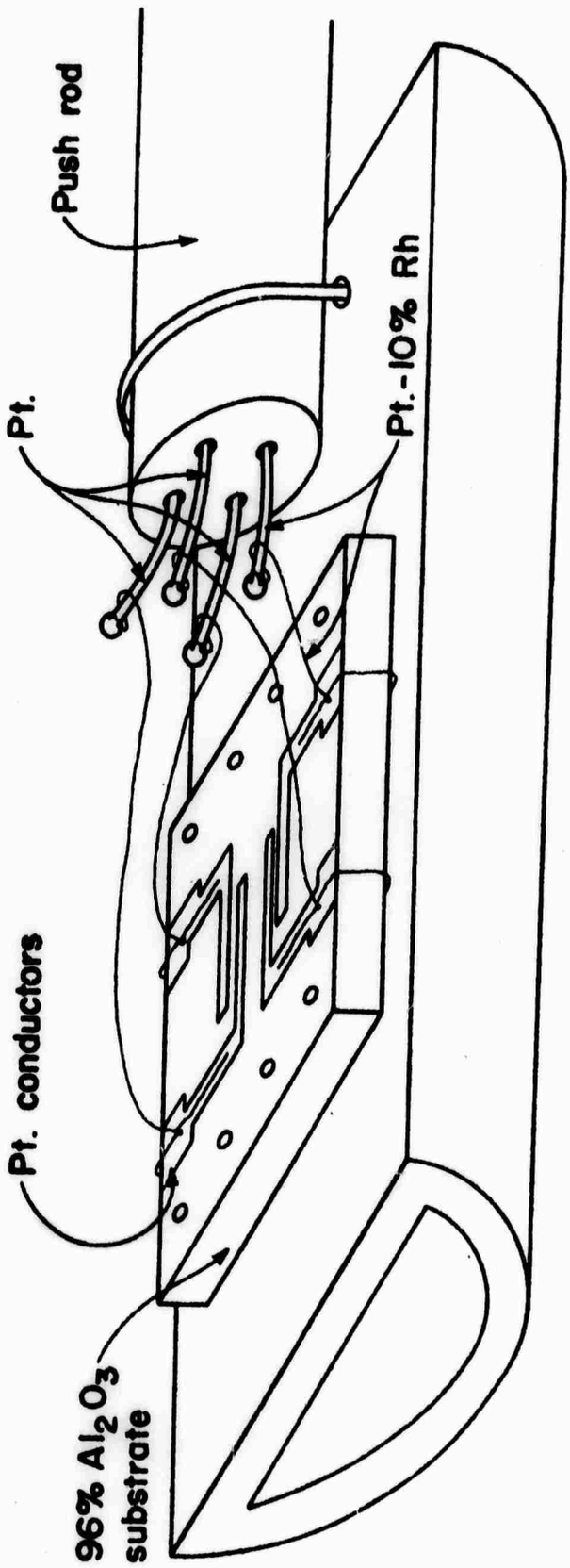

Figure 3. Sample Holder Assembly

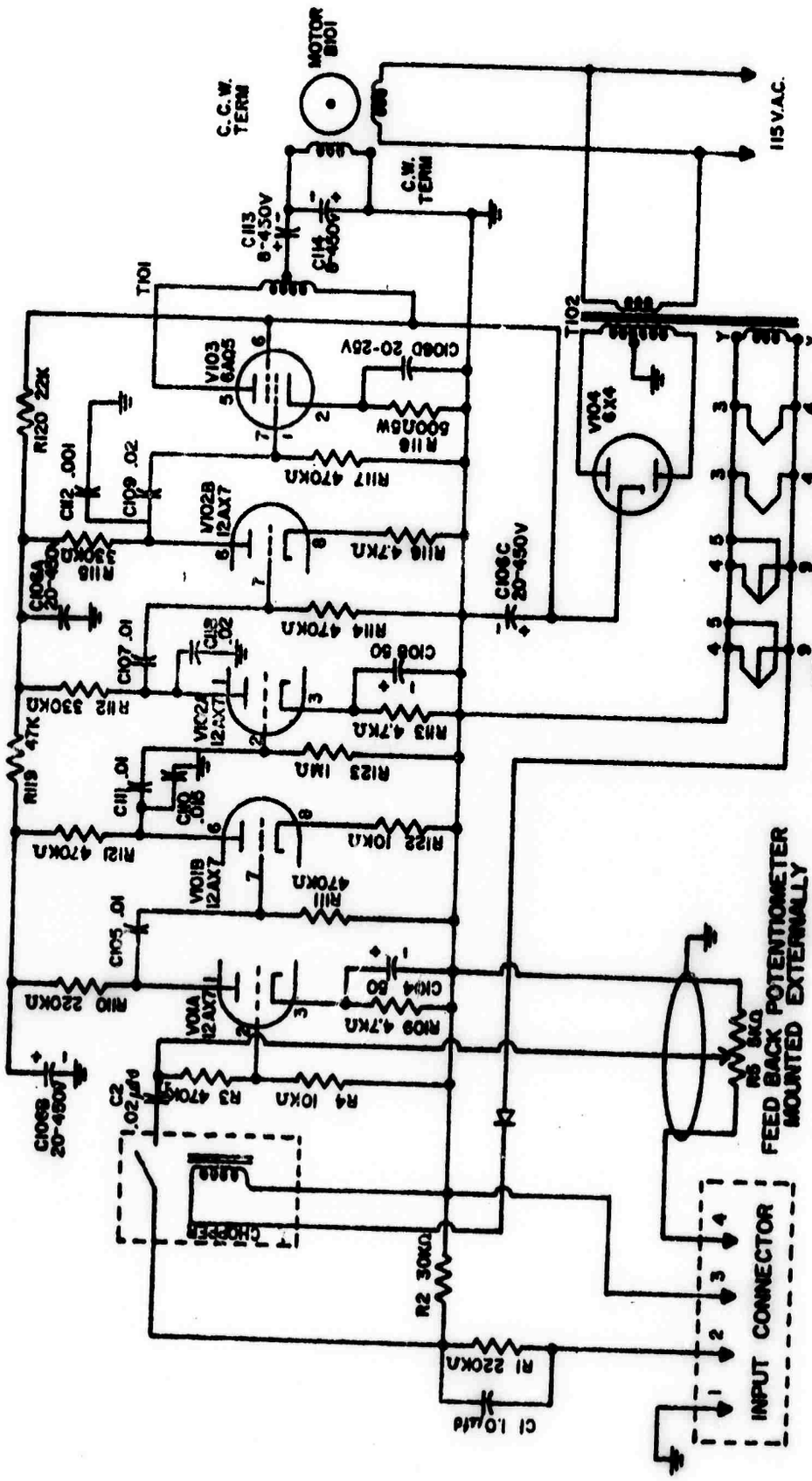

Figure 4. Schematic Diagram of Servo System

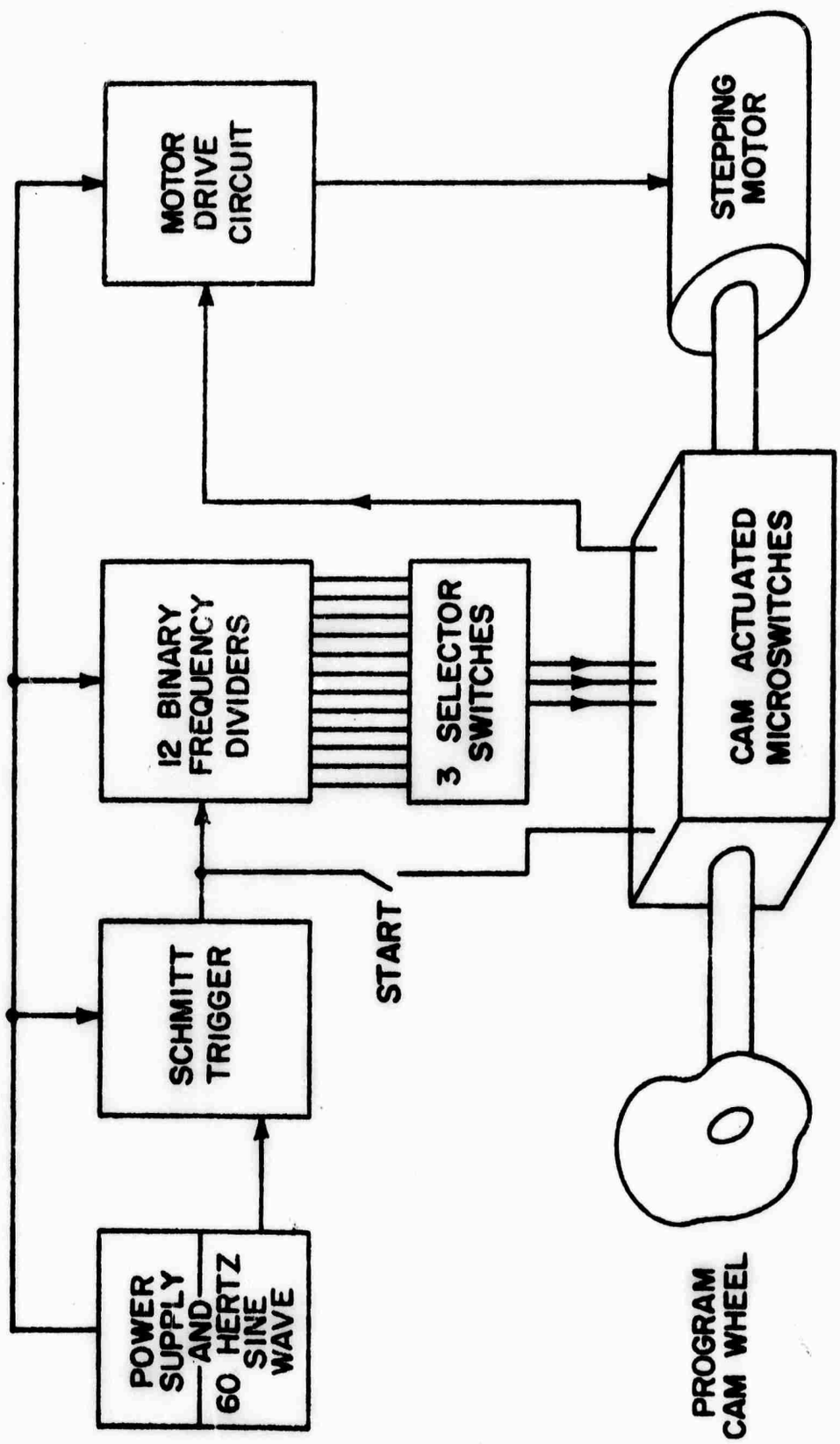

Figure 5. Block Diagram of Cam Drive System

square wave voltages, decreasing in binary steps. The lowest frequency corresponds to 8192 minutes (1 1/2 weeks) rotation time. The twelve lowest frequencies are connected to three twelve position selector switches, wired in parallel so that any of the twelve frequencies is available at each wiper terminal. The angular rate of rotation of the cam wheel is determined by which of the three selector switches is connected to the motor drive circuit.

The shaft for the cam wheel also drives a programmable switch assembly consisting of six SPDT microswitches operated by adjustable cams. The cams are easily adjusted to permit closures of from zero to 360° of shaft rotation. This switch assembly selects which of the three frequencies, determined by the selector switches, controls motor speed and permits the rate of rotation to change anywhere in the program. This feature permits for example, one time-temperature profile to contain rapid rates of temperature change lasting a few minutes as well as constant or slowly varying temperatures lasting several days.

B. Resistance and Temperature Measuring System

A simplified schematic of the resistance and temperature measuring system is shown in Fig. 6. The oscillator, V_s, is a General Radio Model 1310 set to 1000 Hertz, R_s is a variable series resistor to limit the current in the sample, and R_{C1} and R_{C2} represent lead wire resistance plus any resistance of the sample up to the potential leads. V_s and R_s are chosen large enough to approximate a current source. A frequency of 1000 Hz was chosen because reactive effects are negligible for sample resistances encountered, and 1/f noise and 60 Hz interference are minimized. The four terminal measurement technique eliminates the effect of lead wire resistance and contact resistance at the sample.

The resistance recorder is a special version of a Leeds and Northrup Speedmax G. The 9 inch pen motion is divided into three ranges: 0 to 1 mv, 1 to 10 mv, and 10 to 100 mv. Within each range, however, the pen deflection is linear

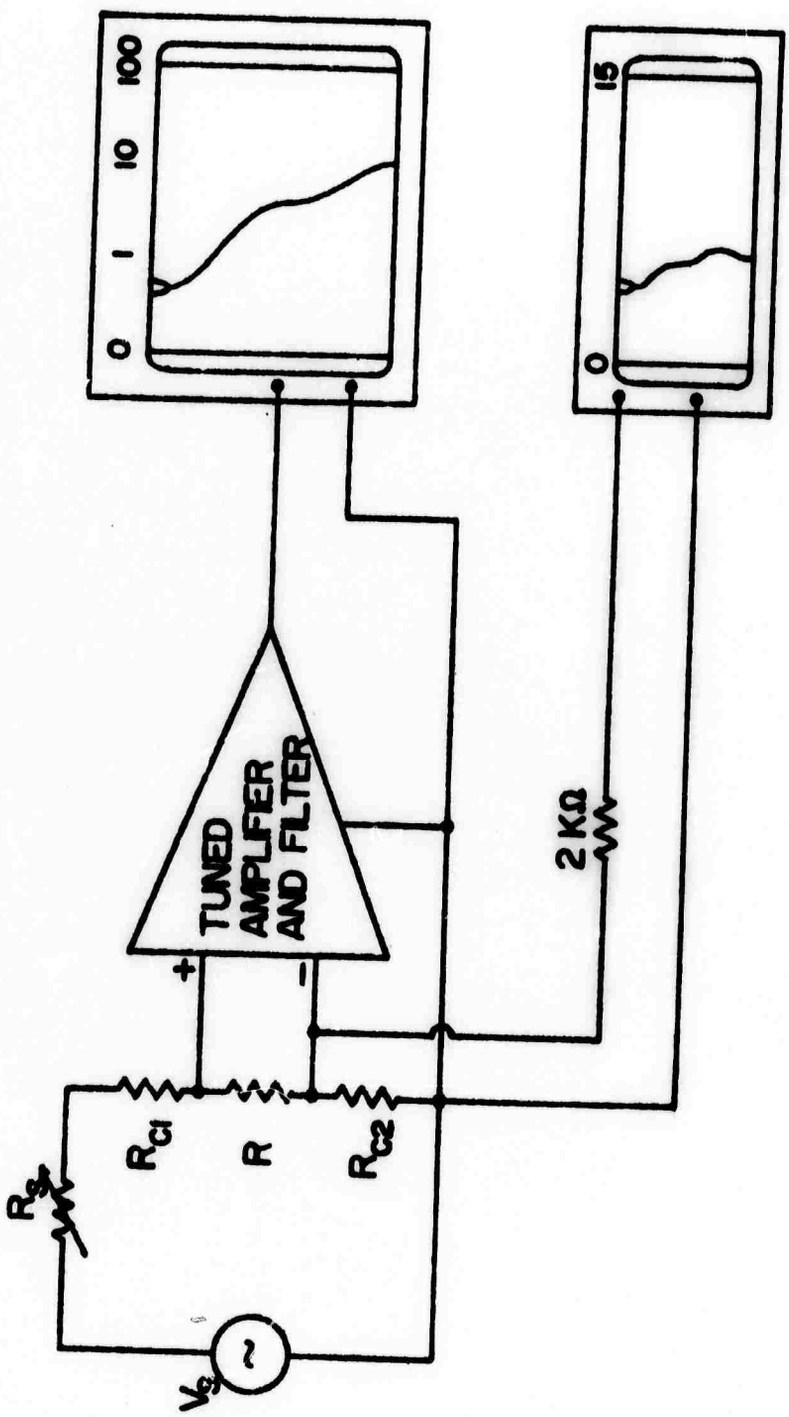

Figure 6. Block Diagram of Resistance and Temperature Measuring System

so that resistance can be recorded over three orders of magnitude without the need for a logarithmic amplifier.

The tuned amplifier and filter shown schematically in Fig. 7 consists of a low noise preamplifier, tuned amplifier, ideal diode, and buffer amplifier and filter. The differential low noise preamplifier uses one-half of a low noise, μA739C operational amplifier. A 22 megohm resistor, not shown, parallels the 68 K ohm resistor to the + input to improve the common mode rejection ratio. The .005μ fd and .01μ fd capacitors are for frequency compensation and provide for stable operation. The gain of this stage should be 34.

The second stage is a tuned amplifier using a μA741C operational amplifier. This amplifier was chosen because of its internal frequency compensation and zero input offset voltage adjustment using the 10K potentiometer. The 62 K Ω resistor and .05μ fd capacitor connected to the + input were chosen for biasing stability and oscillation stability, respectively. The remaining passive components were chosen to give a center frequency gain of 33 and a Q of 10. The Q of 10 was chosen as a compromise between a narrower bandwidth which would have necessitated greater frequency stability of both the amplifier and oscillator, and a wider bandwidth which would have resulted in more noise in succeeding stages

The total gain of the first two stages is about 1000, and permits amplifying low level 1000 Hz voltages to a level where they may be rectified. Rectifying over three orders of magnitude to utilize the capabilities of the chart recorder is difficult, however. For example, if it is agreed that the minimum amplitude of the sine wave should be one volt in order to be somewhat greater than the diodes .6 volt threshold voltage, then the maximum amplitudes must be 1000 v. This is clearly impossible with integrated circuits and unreasonable for any amplifier. Using a maximum sine wave voltage of 5 v and a diode returned to a -.6 volt instead of ground to eliminate the threshold voltage still was inadequate because of the nonlinearity of the diode. Satisfactory performance

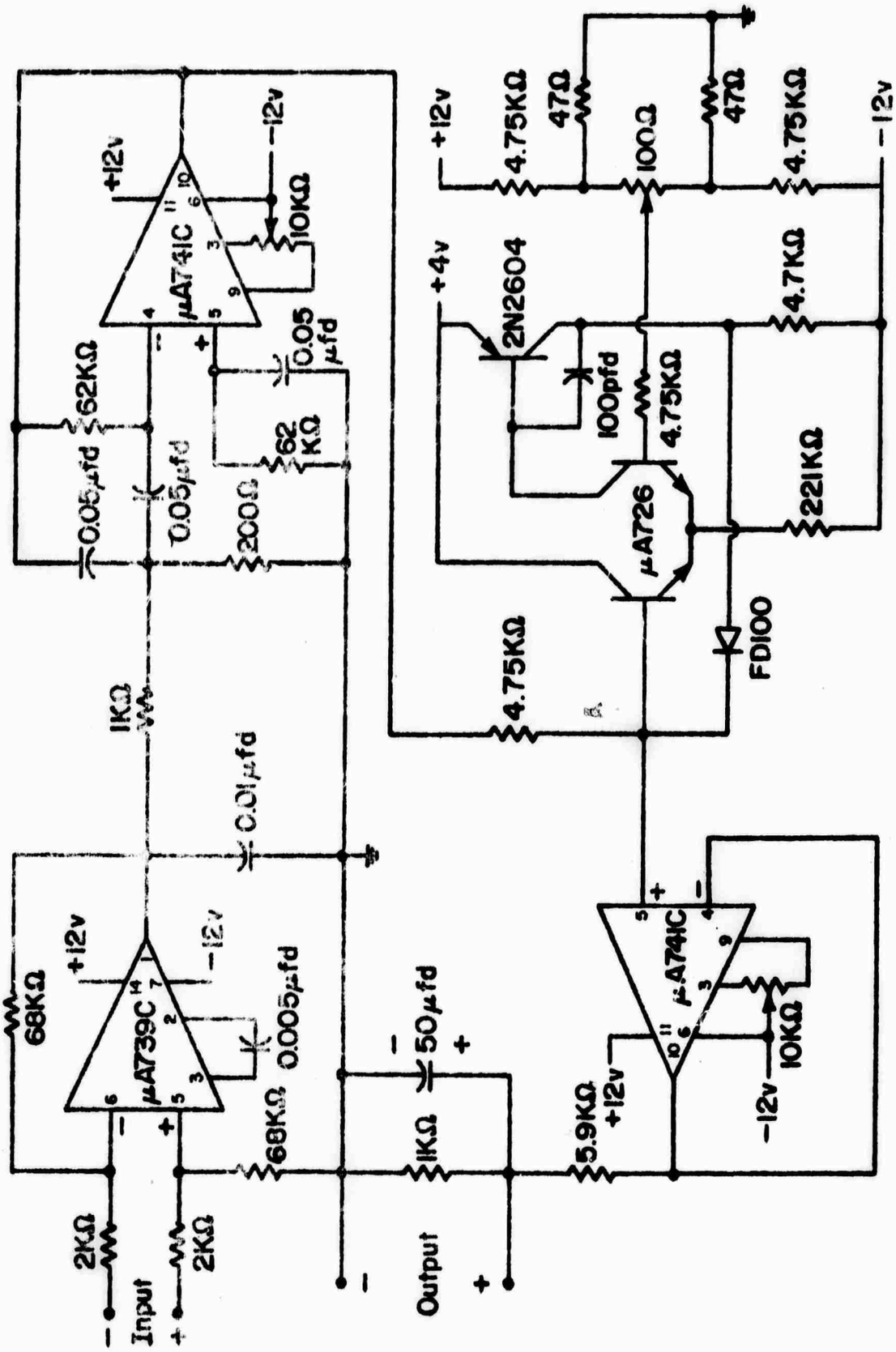

Figure 7. Schematic Diagram of Tuned Amplifier and Filter

was obtained only when an "ideal diode" was constructed. This was accomplished with an ordinary diode and an operational amplifier as shown in Fig. 7. The positive supply voltage was reduced to four volts for this stage to reduce thermal drift due to the different amplitudes of signals. The positive input is connected to a biasing resistor network to facilitate zeroing. The 100 pf capacitor from the collector to the base of the 2N2604-transistor controls the frequency response and latch-up time of the amplifier. Several integrated circuit operational amplifiers were tried for this application but they either were unacceptable because of excessive latch-up time or because of seemingly uncontrollable oscillations.

The fourth stage is a buffer amplifier, attenuator,and low pass filter. The buffer amplifier, a μA741C, serves to minimize loading of the ideal diode, the 6 to 1 attenuator serves to reduce the effects of drift in the second, third, and fourth stages, and the low pass filter is necessary since ordinary chart recorders have a very low input impedance to AC voltages.

Temperature measurement is accomplished simply by adding a chart recorder to the thermocouple leads with a resistor in series to increase the AC input impedance of the recorder. Figure 6 shows this resistor and the connection of the temperature measuring apparatus.

Since all the voltages associated with resistance measurement are sinusoidal, they do not influence the DC voltages due to thermoelectric effects. The chart recorder is not affected by the 1000 Hz oscillations since they are far beyond the frequency response of the recorder.

The resistance and temperature data are recorded on two charts, but neither chart actually records resistance or temperature values. The temperature chart records the thermal EMF of a platinum vs. platinum -10% rhodium thermocouple, and the resistance chart records the output voltage of the amplifier corresponding to the potential drop across both the sample and across a standard

resistor substituted for the sample. A computer program was written to reduce the amount of time required to transform both forms of information into the desired resistance and temperature.

Simultaneous temperature and resistance data points are read by the program. These are easily obtained from the two charts since the time axis of both charts advance the same rate.

To map the EMF values into temperature values a piecewise linear function was used to fit the temperature vs. EMF for the thermocouple.

Although the output of the tuned amplifier and filter is nearly proportioned to the input, there is some lack of linearity over the entire range. To reduce error from this source, a piecewise linear function was specified that calculates the input voltage to the amplifier from the output. Dividing the input voltage by the corresponding standard resistor gives the current due to a particular choice of V_s and R_s in Fig. 6. Sample resistance is then calculated by dividing the input voltages by the current calculated with the standard resistor. Simultaneous resistances and temperatures are printed out on the same line.

C. Sample Preparation

Ruthenium dioxide can be prepared from ruthenium metal or ruthenium compounds. In the case of ruthenium compounds, RuO_2 may be formed by heating in air or by precipitation from an aqueous solution. The primary disadvantage of heating the metal is the long time required for oxidation as discussed in the following section. The oxide first coats the surface and grain boundaries of the metal and then proceeds to form farther into each particle. The compounds of ruthenium permit more rapid oxidation, yielding RuO_2 in no more than a few hours.

The formation of single crystals of RuO_2 was accomplished by vapor transport of the volatile higher oxides. The procedure was to place RuO_2 in a furnace at a temperature sufficient to form RuO_3 and RuO_4. Higher temperatures, forming

predominantly RuO_3, are preferable. The vapor oxides are then transported in a carrier gas of oxygen or air to a cooler region where the volatile oxides decompose to form RuO_2. The temperatures in the furnace and the flow rates of air or oxygen both control the growth rate of the crystals, their size and habit. Three habits have been observed, needle, rod and platelet. The needle and rod are long in the c direction and are the easiest to obtain. The platelets have flat faces in the (011) plane. The largest crystals that have been prepared in our laboratory were about 0.2 mm in diameter and 2 mm long.

Early in the project an attempt was made to prepare samples for measurement of diffusion and solubility of RuO_2 in glass with either an electron microprobe or scanning electron microscope. The procedure was to mount single crystals on wires so electrical measurement could be made, then encapsulate the crystals in glass. It was anticipated that as the crystal dissolved, its resistance would increase. Measuring the resistance vs. time would yield valuable kinetic data and would aid in a more accurate solubility determination. It might also enable observation of a new phase being formed from RuO_2 and glass ingredients.

When samples were prepared with crystals having a diameter of 25-100 microns, no unusual effects could be observed. As measured with the automatic resistance measuring system, the crystals did not change in resistance after substantial periods of time at high temperatures and no change in resistance vs. temperature was observed. If any effects were to be observed, they would be most apparent with crystals of very small diameter. The increase in resistance due to the dissolution of a thin surface layer would be greater and the higher resistance of the small crystals would improve the possibility of observing a new electrically active phase.

The crystals used for experiments reported in Section III varied in diameter from about 2 microns to about 3.5 microns and had a length from about

1 mm to about 1.5 mm. The crystals were mounted on four 1 mil platinum wires bonded to conductive pads in a recessed area of an alumina substrate (see Fig. 8a). Preparing a sample involved selecting a crystal, transporting it to mounting wires, positioning it in the desired location and cementing the crystal to the four wires with the platinum paste. The crystal was then encapsulated in glass. A mounted crystal without glass is shown in Fig. 8b. The entire procedure required a steady hand and good luck.

The crystal was mounted in a recessed area of the substrate so that the glass could be contained better in the vicinity of the crystal. The glass could not be added by covering the crystal with powder. As discussed in Section III, the glass sinters and undergoes a volume shrinkage at 600°C when the viscosity is still high. This can break the crystal and remove the cemented wires. A procedure that produced better results was to add the glass to the well in the substrate by placing the powder around the side of the well to form a cone shape with no glass in contact with the lead wires, and then fire to 700°C for a short time to cause the volume shrinkage. This procedure would then be repeated three or four times until a conical shape of fired glass extended from near the crystal to the rim of the well. When this point was reached, the sample was heated to 800°C or above where the glass became low enough in viscosity to flow to the center and encapsulate the crystal by rising up around it. Once the crystal was encapsulated, the well could be filled by adding powder and heating to 700°C. Once the well was filled it was found to be desirable to cover it with a disk of alumina to retard the flow of glass out on to the substrate at high temperatures. A small hole in the center of the disk made it possible to observe the crystal and the level of glass and to add more glass when necessary.

One major problem was encountered with this technique. When the glass rises to encapsulate the crystal the surface tension pulls the crystal and wires down

a. Recess in Substrate with 1 mil Platinum Wires Attached

b. Mounted RuO_2 Single Crystal

Figure 8. Mounting of Small RuO_2 Single Crystals

closer to the substrate surface. Because the potential-current lead pair originally formed a triangle with the bottom of the well, lowering the crystal causes strains that sometimes break the crystal or rupture a lead-to-crystal bond. This problem can be solved by using four wires during attachment but cementing only two. The measuring circuit could still be four wires up to the crystal leads, and hence eliminate the effect of the several ohms of lead wire resistance.

III. Results and Discussion

A. Characterization of Ingredient Materials

To maintain the greatest simplicity in all resistor experiments the number of ingredient materials has been limited to five; alumina substrate, lead borosilicate glass, ruthenium dioxide, platinum conductive paste, and wires for crystal mounting and connections to the substrate. The wires used for mounting single crystals of RuO_2 were "chemically pure" annealed gold wire in early portions of the experiments and chemically pure annealed platinum wires later. The wires used for connections to the substrate for electrical measurements, as shown in Fig. 3, were platinum and platinum - 10% rhodium. The remaining four materials are more likely to influence the behavior of any experimental sample. Therefore, they have been characterized more thoroughly and are discussed in this section.

1. Substrates

The ceramic substrate chosen for this work was 96 percent alumina. This material was selected because it is common to the thick film technology, it seemed adequate for all experiments, and it is low in cost. More specifically, the substrates are made from AlSiMag 614 alumina and have a shape commonly referred to as the 12 pin SLT substrate. The substrates were supplied by the American Lava Corporation with the permission of the IBM Corporation.

This shape substrate (0.5 x 0.5 x 0.060 inches) seemed well suited to the experiments; the area dimensions of the substrate are large enough for all samples and are compatible with the substrate fixture of the furnace. The substrates are thicker than typically used throughout the industry. A more typical thickness might be .020-.025 inches, but the thicker substrates have a higher transverse thermal conductance that promotes more uniform temperatures in the linear gradient of the furnace. The thicker substrate should also more

completely dominate the expansion vs. temperature of the thinner thick film resistor, and the thicker substrates made it possible to form a recessed area in the center of the substrate to be filled with glass.

Table I lists the published characteristics of AlSiMag 614 alumina. To further characterize the material a chemical analysis was obtained. The results are shown in Table II. An average coefficient of thermal expansion such as given in Table I is insufficient to establish the influence of thermal stress on resistor performance. Therefore, the expansion of the AlSiMag 614 was measured as a function of temperature; the results are shown in Fig. 9.

2. Glass

A lead borosilicate glass having a composition of 63% PbO, 25% B_2O_3, and 12% SiO_2 was chosen for this work for the following reasons:

1. It is known that this glass plus RuO_2 will produce good resistors.
2. It has a low softening temperature (480°C).
3. The physical properties of the lead borosilicate glass system have been rather thoroughly studied.
4. It is possible to vary the coefficient of thermal expansion by varying the ratios of the three ingredients.

Ingredient materials were mixed together, heated in a clay crucible, poured into water, ball milled, and sieved to obtain particles that would pass through a 325 mesh screen. The surface area of the glass powder was measured by a BET method and found to be 1.25 m^2/gram. The particle size calculated from surface area depends on the density of the glass. Based on an assumed density of 4.65 grams/cm^3 the average particle size is a cube with an edge of 1.03 microns.

The expansion vs. temperature was measured and is shown in Fig. 10. The thermal coefficient of linear expansion from room temperature to 300°C is 6.96 x 10^{-6}/°C. The contraction at about 350°C is partially due to the force of the measuring system.

Table I. Thermophysical Properties of AlSiMag 614, 96% Al_2O_3

Property	Unit			
Water Abosrption	%		0 Impervious	
Specific Gravity	---		3.70	
Hardness	Mohs' Scale		9	
	Rockwell 65 N		78	
Thermal Expansion Linear Coefficient	Per °C	25-300°C	6.4×10^{-6}	
		25-700°C	7.5×10^{-6}	
		25-900°C	7.9×10^{-6}	
Tensile Strength	Psi	Kg/cm^2	25 000	1 760
Compressive Strength	Psi	Kg/cm^2	375 000	26 360
Flexural Strength	Psi	Kg/cm^2	46 000	3 230
Resistance to Impact	Inch-lbs.	Meter-Kg	7.0	.081
Modulus of Elasticity	Psi x 10^6	$Kg/cm^2 \times 10^6$	47	3.30
Shear Modulus	Psi x 10^6	$Kg/cm^2 \times 10^6$	19	1.34
Poisson's Ratio	---		.22	
Thermal Conductivity 25°C	BTU in./ hr. ft^2 °F	cal. cm./sec. cm^2 °C	244	.084
Thermal Conductivity 300°C			119	.041
Thermal Conductivity 500°C			75	.026
Thermal Conductivity 800°C			58	.020
Dielectric Strength 60 Hertz AC Test Discs 1/4" thick	volts per mil	Kilovolts per mm	210	8.3
Volume Resistivity 25°C	Ohm-centimeters		$>10^{14}$	
Volume Resistivity 100°C			2.0×10^{13}	
Volume Resistivity 300°C			1.1×10^{10}	
Volume Resistivity 500°C			7.3×10^{7}	
Volume Resistivity 700°C			3.5×10^{6}	
Volume Resistivity 900°C			6.8×10^{5}	

		25°C	300°C	500°C	800°C
Dielectric Constant[e]	1 MHz	9.3	9.5	10.8	22.4
Dissipation Factor[e]	1 MHz	.0003	.0027	.0131	.0911
Loss Factor[e]	1 MHz	.0028	.0257	.1415	2.041

Table II. Chemical Analysis of AlSiMag 614 Substrate

Element	ppm(wt)
Ba	20
Fe	500
Mn	5
Mg	6000
Na	2000
Ga	200
Ni	5
Ti	200
Li	10
Cr	10
Sn	<10
Cu	<5
Co	<5
Mo	<10
U	<10
Zr	<30
K	1000
Ca	1500
Si	10,000

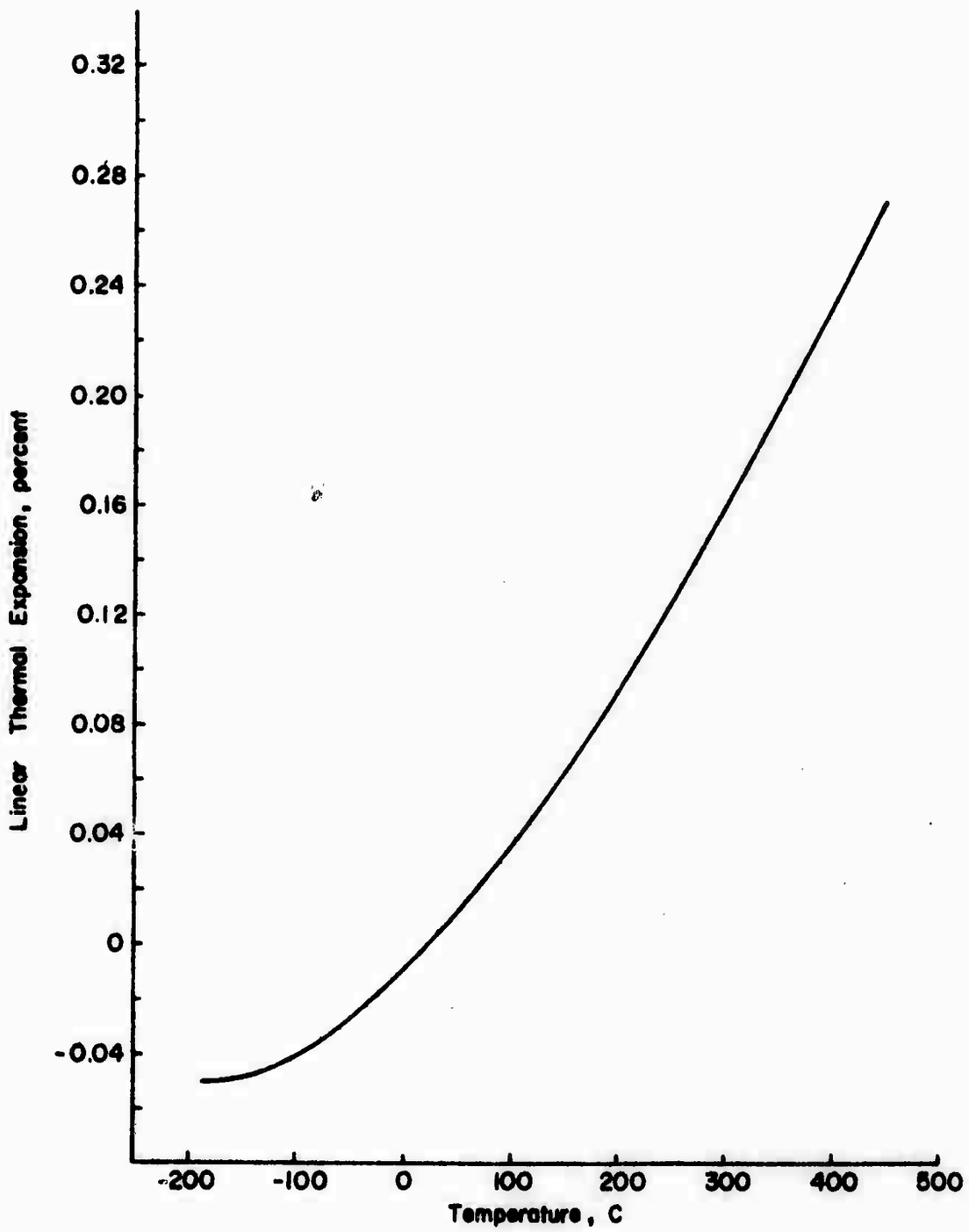

Figure 9. Thermal Expansion of AlSiMag 614 Substrate

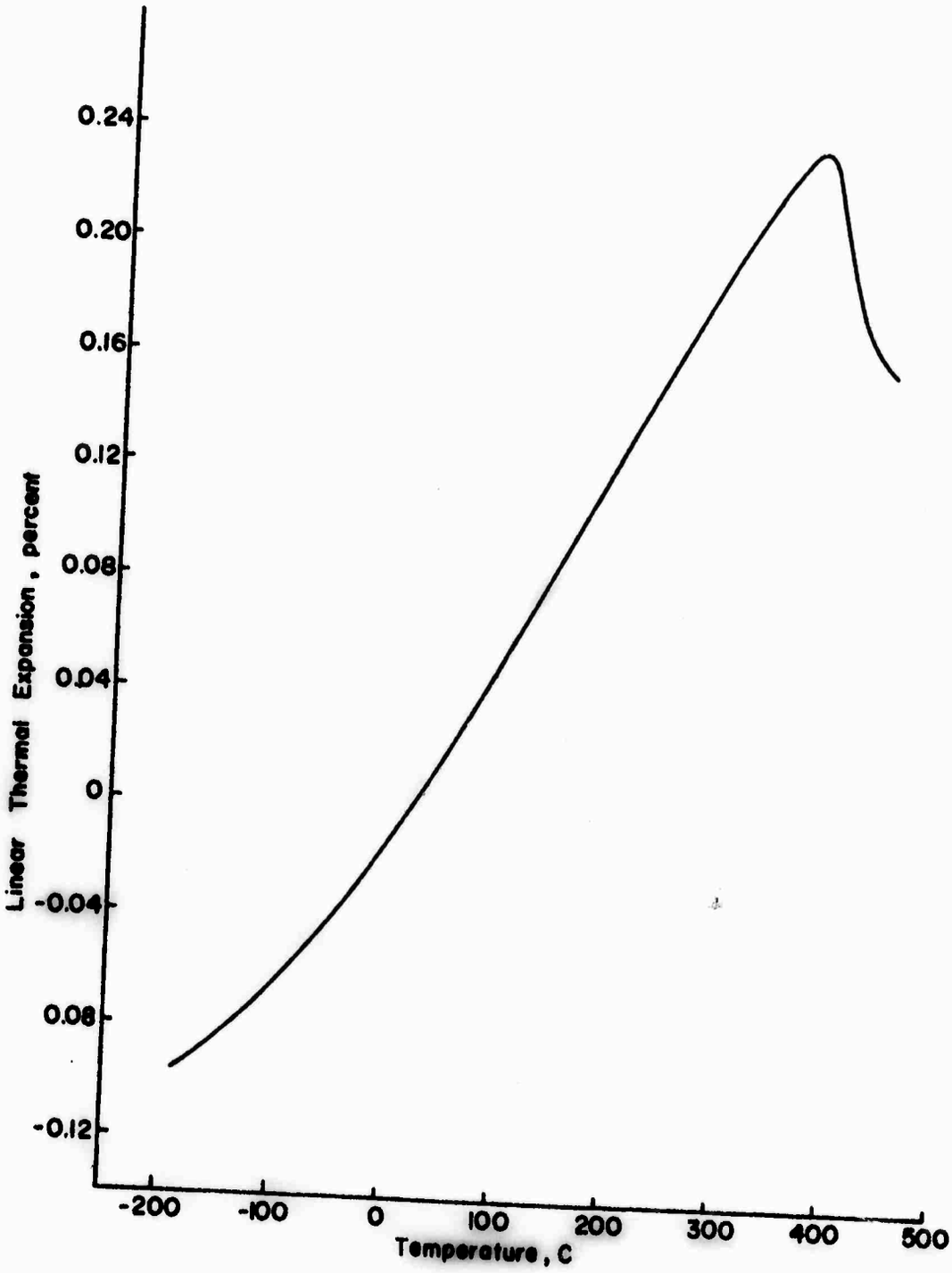

Figure 10. Thermal Expansion of Lead-borosilicate Glass

A chemical analysis of the glass was obtained in order to determine complete composition. The major and minor constituents, determined by wet chemical and spark mass spectrographic methods respectivity, are shown in Table III. The sum of the percentages is 100.9 representing the approximately 1% error common in wet chemical analysis. The alumina and excess silica probably originated from the clay crucible.

In the course of conducting experiments several observations of sintering, flowing, and wetting were made that are helpful in preparing samples and anticipating performance. If the glass is heated between 30 and 120°C/minute to about 600°C, the powder sinters into an irregular shaped solid, heavily filled with air bubbles, that is milky white in color. Heating to 700°C at similar rates results in a smooth surface that wets to the substrate but still contains air bubbles near the surface and does not flow significantly in a few minutes. Heating to 800°C produces a clear, bubble free glass that creeps out on to the substrate about .05 inches in a few minutes even when the glass was originally in a recession, below the surface of the substrate. Heating to 900-1000°C results in a more rapid creep rate of the glass onto the surface and eventually almost empties the recessed area in a duration of several minutes. The glass that creeps out onto the substrate at 1000°C is often thin enough to show the texture of the substrate surface.

3. Conductive Paste

Conductive patterns on the substrate and adhesion of crystals to wires were both established with Englehard 6082 fluxed platinum paste. It was chosen because of its moderately good adhesion and electrical resistance, and because it is moderately stable and unreactive at high temperatures. A chemical analysis of the paste after firing to remove the organics is shown in Table IV. As can be seen, the flux is Bi_2O_3.

Table III. Chemical Analysis of Lead-borosilicate Glass

Major Constituents

Oxide	PbO	B_2O_3	SiO_2	Al_2O_3	Bi_2O_3
Percent	62.6	24.4	12.3	1.0	0.6

Minor Constituents

Element	ppmw	Element	ppmw
Li	10.	In	<0.2
Be	<0.05	Sn	1.
F	10.	Sb	≤0.1
Na	400.	Te	≤0.1
Mg	200.	I	<0.02
P	3.	Cs	0.3
S	3.	Ba	3.
Cl	20.	La	≤0.1
K	300.	Ce	≤0.1
Ca	100.	Pr	≤0.03
Sc	0.3	Nd	<0.1
Ti	30.	Sm	<0.1
V	0.6	Eu	<0.06
Cr	2.	Gd	<0.1
Mn	100.	Tb	<0.03
Fe	100.	Dy	<0.1
Co	≤0.1	Ho	<0.03
Ni	1.	Er	<0.1
Cu	150.	Tm	<0.03
Zn	4.	Yb	<0.1
Ga	1.	Lu	<0.03
Ge	<0.5	Hf	<0.1
As	<0.1	Ta	≤0.3
Se	<0.2	W	≤0.1
Br	0.3	Re	<0.05
Rb	5.	Os	<0.07
Sr	0.5	Ir	<0.05
Y	0.2	Pt	<0.1
Zr	3.	Au	<0.1
Nb	0.06	Hg	<0.1
Mo	<0.2	Tl	≤0.4
Ru	<0.2	Th	≤0.5
Pd	<0.2	U	<0.2
Ag	3.		
Cd	<0.3		

Table IV. Analysis of Platinum Paste (Engelhard #6082)
(Inorganic Components)

	values in ppma		
Element	Paste	Element	Paste
Li	1	Mn	10
B	5	Fe	350
F	10	Co	5
Na	1500	Ni	<15
Mg	100	Cu	15
Al	100	Zn	50
Si	150	Sr	2
P	3	Rh	20
S	100	Pd	30
Cl	500	Ag	10
K	30	Ba	15
Ca	50	Au	20
Sc	1	Pb	10
Ti	30	Bi	0.3-1.0%

All other impurities < 1 ppma.

Experience has shown that this paste adheres well to a large variety of ceramic materials provided an adequate technique is used. Particularly with the first application, it is easy, for some ceramic materials, to apply the paste too thick. If the thick paste is dried and fired too quickly a dry film may form on the surface that will be disrupted by volatile materials lower in the film leaving rapidly. This type of failure can be eliminated by more gradual drying and firing. A second mode of failure results from the two stages of coalescence of the conductive. The first volume shrinkage occurs during drying and as most of the organics leave, the particles of material cohere. If the adhesion of the partially wet film to the substrate material is not adequate, the dimensional changes during drying will cause the conductive film to separate from the substrate as it shrinks. The second volume reduction occurs at high temperature as the platinum sinters in the presence of the flux. Again, if the adhesion to the substrate is not adequate at this stage, the dimensional changes of the film will cause it to separate. The best solution to this problem is to apply the film as thin as possible. Once an adhered layer is formed less care is required for additional layers. In general a smooth surface such as crystal faces have the lowest adhesion, more textured surfaces, such as an established film of 6082, are best. The texture of the 96% alumina substrates are intermediate in quality in this respect.

An interesting effect occurs with the combination substrate, glass, and 6082 conductive. At high temperatures (>800°C) the glass causes the metal film to separate from the substrate and float in the glass. It does not float to the surface and does not move significantly. Thus far, it has not caused any significant problems.

4. Ruthenium Dioxide

Ruthenium dioxide was chosen as the conductive material for the thick film resistors because reports of its successful use are ample, its physical

properties are reasonably well defined, and it is stable to sufficiently high temperatures. Compared to the other materials used in this project, a relatively large amount of information has been reported on the thermophysical properties of RuO_2, most of it in the last decade. This has resulted in a partially complete understanding of the material, but many details are still missing or not yet resolved.

Ruthenium dioxide has the tetragonal rutile crystal structure with two formula units per unit cell. Several authors [10-14] have recently reported unit cell dimensions as shown in Table V. It can be seen that RuO_2 contracts in the c direction with increasing temperature. That is, it has a negative coefficient of linear thermal expansion (α). Expansion vs. temperature is a non-linear relationship, and so $\alpha_{||}$ and $\alpha_{\perp}$ (parallel and perpendicular to the c axis) are functions of temperature. Based on their measurements, Rao and Iyengar [13] have developed mathematical expressions for $\alpha_{||}$ and $\alpha_{\perp}$. The formulas are:

$$\alpha_{||} = -1.248 \times 10^{-6} - 5.392 \times 10^{-9} T - 2.273 \times 10^{-12} T^2$$

and

$$\alpha_{\perp} = 6.447 \times 10^{-6} + 1.920 \times 10^{-8} T - 1.075 \times 10^{-11} T^2$$

where T is the temperature in C°. They indicate that values of $\alpha_{||}$ and $\alpha_{\perp}$ calculated with these formulas agree to within a few percent of the observed values.

The value of α in any direction may be calculated from $\alpha_{||}$ and $\alpha_{\perp}$ by the formula:

$$\alpha(h,k,\ell) = \left[\frac{h^2+k^2}{a^2} \alpha_{\perp} - \frac{\ell^2}{c^2} \alpha_{||} \right] \Bigg/ \left[\frac{h^2+k^2}{a^2} + \frac{\ell^2}{c^2} \right]$$

where h, k, ℓ are the Miller indices of the direction.

Although knowledge of $\alpha_{||}$ and $\alpha_{\perp}$ is valuable information for some types of experiments, it is not directly useful when RuO_2 powder is used, such as in

Table V. Crystal Data for Ruthenium Dioxide

	Temperature (°C)	Lattice Parameters (Å)	
		a	b
Cotton and Mague 1966	RT	4.491±.007	3.107±.005
Fletcher, et al. 1968	RT	4.4904±.0001	3.1064±.0001
	190	4.4971	3.1055
	400	4.5074	3.1031
	605	4.5204	3.1002
	795	4.5342	3.0963
Shannon, 1968	RT	4.4906±.0002	3.1064±.0002
Rao and Iyengar 1969	30	4.4909±.0003	3.1064±.0004
	165	4.4958	3.1062
	267	4.5003	3.1051
	361	4.5053	3.1037
	461	4.5109	3.1033
	563	4.5198	3.1012
	608	4.5198	3.1008
	702	4.5258	3.0995
Bowman 1970	RT	4.4919±.0008	3.1066±.0007

thick film resistor formulations. This is because of the random orientation of the small crystals. What is required is an average value of elongation vs. temperature based on volume expansion. This is calculated by the formula

$$\text{Percent elongation (T)} = 100\left[V^{1/3}_{(T)} - V^{1/3}_{(RT)}\right]/V^{1/3}_{(RT)}$$

where V(T) is the volume at temperature T, and V(RT) is the volume at room temperature. Table VI shows the volume of a unit cell and the average elongation calculated with the above equation. The data of both Rao and Iyengar [13] and Fletcher, et.al., [12] have been used. In the calculations, the a parameter was assumed to be 4.4905Å. This was chosen based on the values reported by Shannon [12] and by Fletcher, et.al. [11]. The elongation vs. temperature determined from lattice parameter measurements are important because crystals of a size sufficient for accurate dilatometer measurements have not been grown.

Several investigations of the chemistry of the ruthenium-oxygen system have been reported dealing with both the thermodynamic properties of RuO_2, and with the formation of other oxides [15-20]. Table VII summarizes the thermodynamic properties of RuO_2 extrapolated to 298°K. A variety of experimental procedures were used to obtain these data including galvanic cell, thermobalance, and static pressure methods. Although the differences in the reported values of ΔG°_{298} are greater than the individual estimated errors, the agreement to within about one kilocalorie is good.

All the values reported in Table VII were calculated from data measured at higher temperatures. Figure 11 compares these data by showing values of the standard free energy of formation, ΔG°, at the measurement temperatures. The data of Chatterji and Vest [20] parallels the data obtained at higher temperatures but is lower; this may be partially due to the $\alpha \rightarrow \beta$ transformation in ruthenium metal at 1308°K. The data of Fizzini and Rossi shows less agreement.

Figure 12 shows the phase fields for the Ru-RuO_2 system over the temperature range 600-1500°C. This phase diagram is essential for considerations of the

Table VI. Thermal Expansion of Ruthenium Dioxide

Temperature (°C)	Unit Cell Volume ($Å^3$)	Percent Elongation
22	62.64	---
30	62.65	0.0594
165	62.78	0.0765
190	62.81	0.0883
267	62.87	0.1315
361	63.00	0.1906
400	63.04	0.2152
461	63.15	0.2693
563	63.28	0.3414
605	63.35	0.3765
608	63.34	0.3741
702	63.49	0.4489
795	63.66	0.5385

Table VII. Thermodynamic Properties of Ruthenium Dioxide at 298°K

Investigator		ΔH°_{298} (kcal/mole)	ΔS°_{298} (e.u.)	ΔG°_{298} (kcal/mole)	S°_{298} (e.u.)
Bell and Tagami	[15]	-72.2±2.0	-43.3±2.0	-59.3±2.6	12.5±2.0
Shchukarev and Ryabov	[16]	-72.4±.4	---	---	---
Shafer, et.al.	[17]	-71.2	-41.4	-58.9	14.5
Pizzini and Rossi	[18]	-73.36±.35	-41.88±.46	---	---
Latimer	[19]	---	---	---	14.5
Chatterji and Vest	[20]				
Extrapolated		-71.44±.19	-38.97±.1	-58.84±.12	16.93±.1
Corrected		-72.43±.2	-40.44±.2	-60.38±.2	15.46±.2

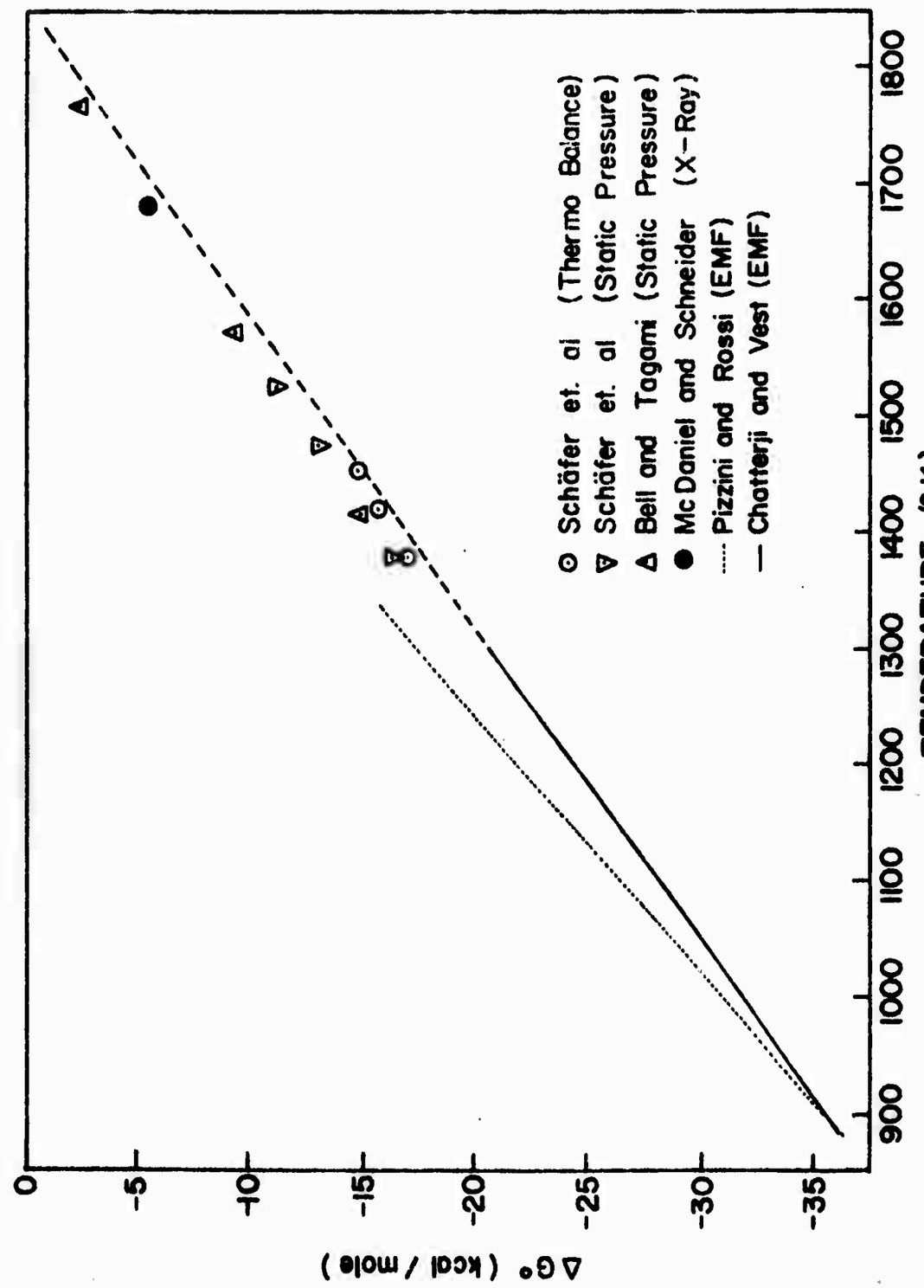

Figure 11. Standard Free Energy of Formation of RuO_2

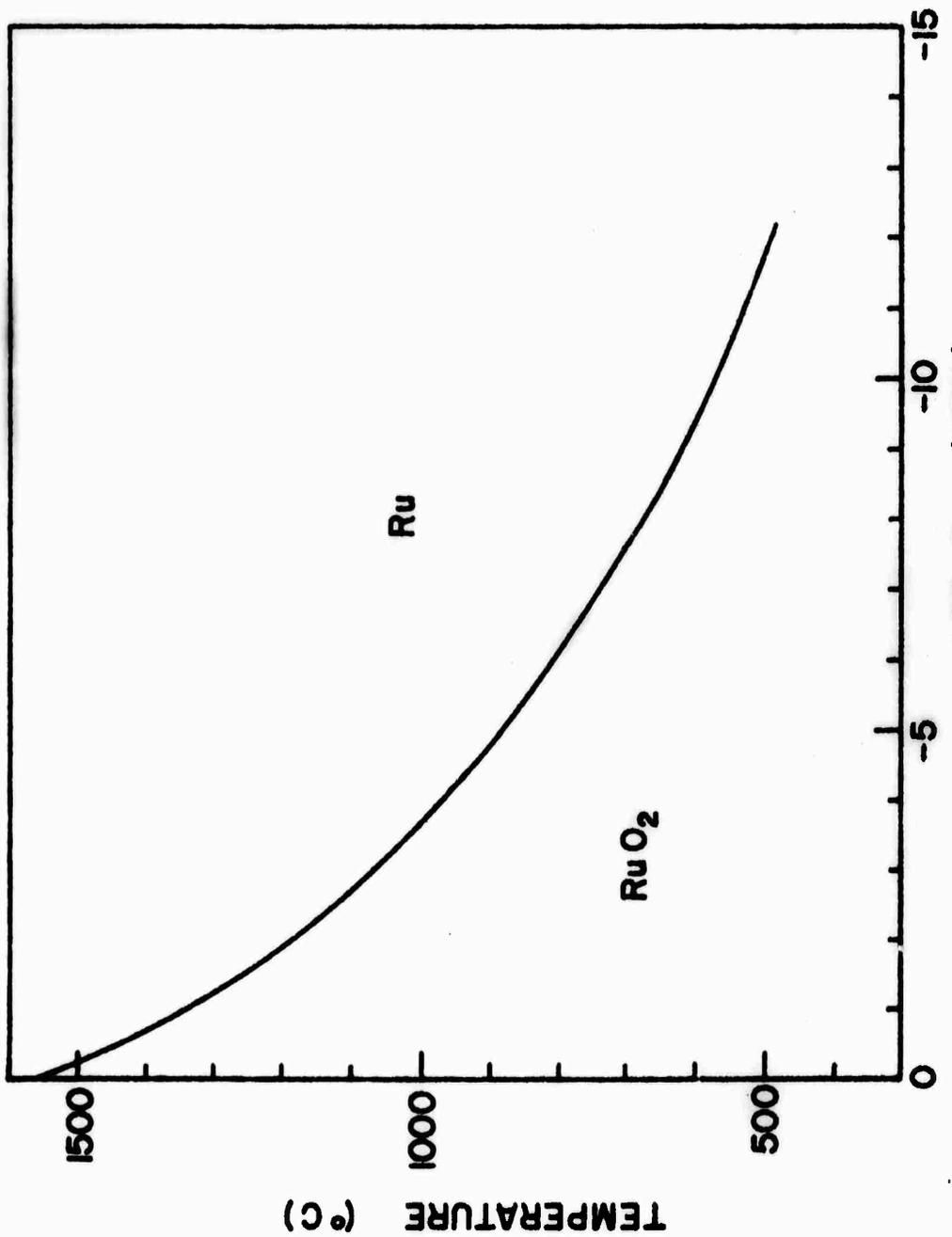

Figure 12. Phase Fields for the Ru-RuO_2 System

oxygen partial pressures and temperatures during thick film resistor firing. For example, if at 800°C (a possible temperature for preparing RuO_2 thick film resistors) the partial pressure of oxygen within the film is below 10^{-6} atmospheres, the RuO_2 will be reduced to ruthenium metal. The oxygen partial pressure in the film will be a function of at least the kiln atmosphere and the rate of heating.

Of course, thermodynamics can not predict the rate at which oxidation-reduction reactions such as $Ru + O_2 \rightleftharpoons RuO_2$ will occur. However, it has been experimentally observed that ruthenium metal oxidizes very slowly. For example, we observed that heating ruthenium metal powder at 1200°C for one hour and at 900°C for 12 hours resulted in 19% oxygen content as compared to 24% required for RuO_2. Similarly, Bell and Tagmani [15] heated the metal several days at 950°C to get within 1% of the theoretical value. The slow rate of oxidation could lead to erroneous conclusions. For example, Iles' report that RuO_2 frequently has a significant oxygen deficiency could have resulted from weight gain measurements of the metal when only partial oxidation occurred. The same is true of Sartain's conclusion concerning the existance of Ru_2O_3. In all of the recent thermodynamic work no evidence has been found that there are any anhydrous oxides between Ru and RuO_2. When ruthenium has been thoroughly oxidized there have been small differences in the ratio of ruthenium to oxygen ($\leq \pm 1\%$). This suggests that RuO_2 might be a stable material over some range of oxygen to ruthenium content.

The reduction of RuO_2 to ruthenium metal is much more rapid than the oxidation of the metal. RuO_2 can be quantitatively reduced in a hydrogen atmosphere in about 5 minutes at 125°C, or in carbon monoxide in about 5 minutes at 300°C

When RuO_2 is heated to sufficiently high temperatures, two volatile oxides are formed, RuO_3 and RuO_4. At high temperatures both these oxides are in the vapor phase although RuO_4 has been prepared as a liquid at room temperature.

Based on transpiration measurements by Bell and Tagmani [15] the partial pressures of RuO_3 and RuO_4 above RuO_2 exposed to air were calculated as functions of temperature; the results are shown in Fig. 13. As can be seen, RuO_3 predominates at higher temperatures. The weight loss of RuO_2 due to the formation of these volatile oxides was measured as a function of temperature. The specific surface area of the powder used for these measurements was 15.0 m^2/gm as determined by the BET method. Fig. 14 shows the rate of weight loss per square meter of surface area; for this particular powder the rate of weight loss in air was 0.01 percent/min at 850°C. These vaporization data are important because the possibility of RuO_2 loss from thick film resistors during processing must be considered.

The most extensive measurements on the electrical resistivity of RuO_2 have been reported by Ryden et. al. [21] from below 4.2°K to 1000°K with several crystals, most of which had residual resistance ratios of 20-50. Based on the results three conclusions are stated: RuO_2 behaves electrically as a transition metal, Matthiesen's rule is not obeyed, and the resistivity of RuO_2 is isotropic. Each of these conclusions will now be discussed.

The conclusion that RuO_2 behaves as a transition metal was based on the ability to fit the resistivity data with the following function for a two band metal for the proper choice of parameters.

$$\rho(T) = \rho_o + \rho_2 T^2 + \rho_3 T^3 \left[J_3(\theta_D/T) - J_3(\theta_E/T)\right] \qquad (3)$$

In Eq. (3) ρ_o is the residual resistivity, $\rho_2 T^2$ represents interband electron-electron scattering, and the last term represents interband electron-phonon scattering, where θ_D is the Debye temperature and θ_E is the Wilson temperature. Use of Eq. (3) assumes that the intraband electron-phonon scattering which predominates in a one band metal such as copper is negligable in RuO_2.

Fig. 15 shows the data points reported by Ryden, et.al. compared to the values of $\rho(T)$ calculated with Eq. (3) using their reported parameters (dashed line).

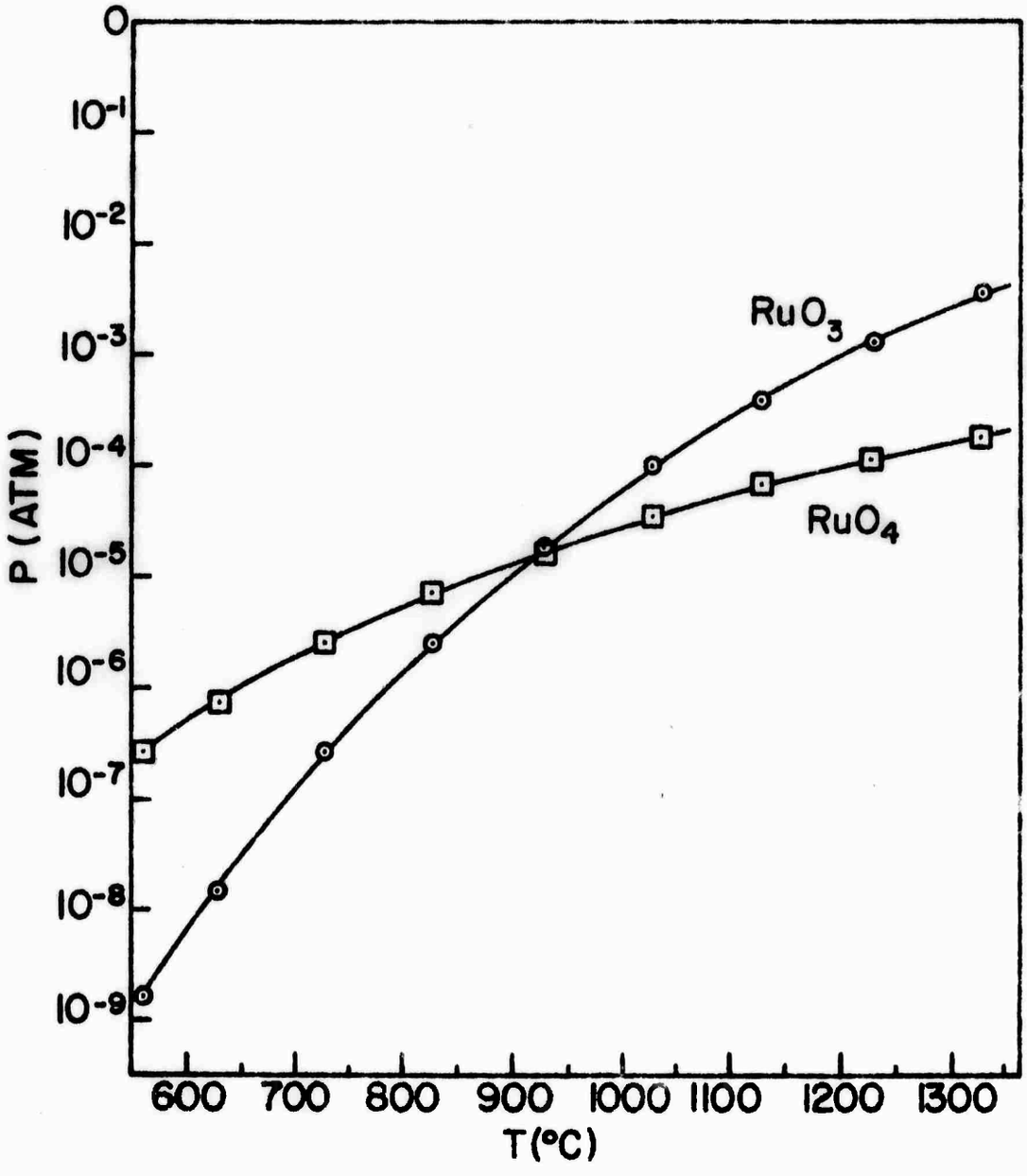

Figure 13. Partial Pressure of $RuO_3(g)$ and $RuO_4(g)$ over $RuO_2(s)$ in Air

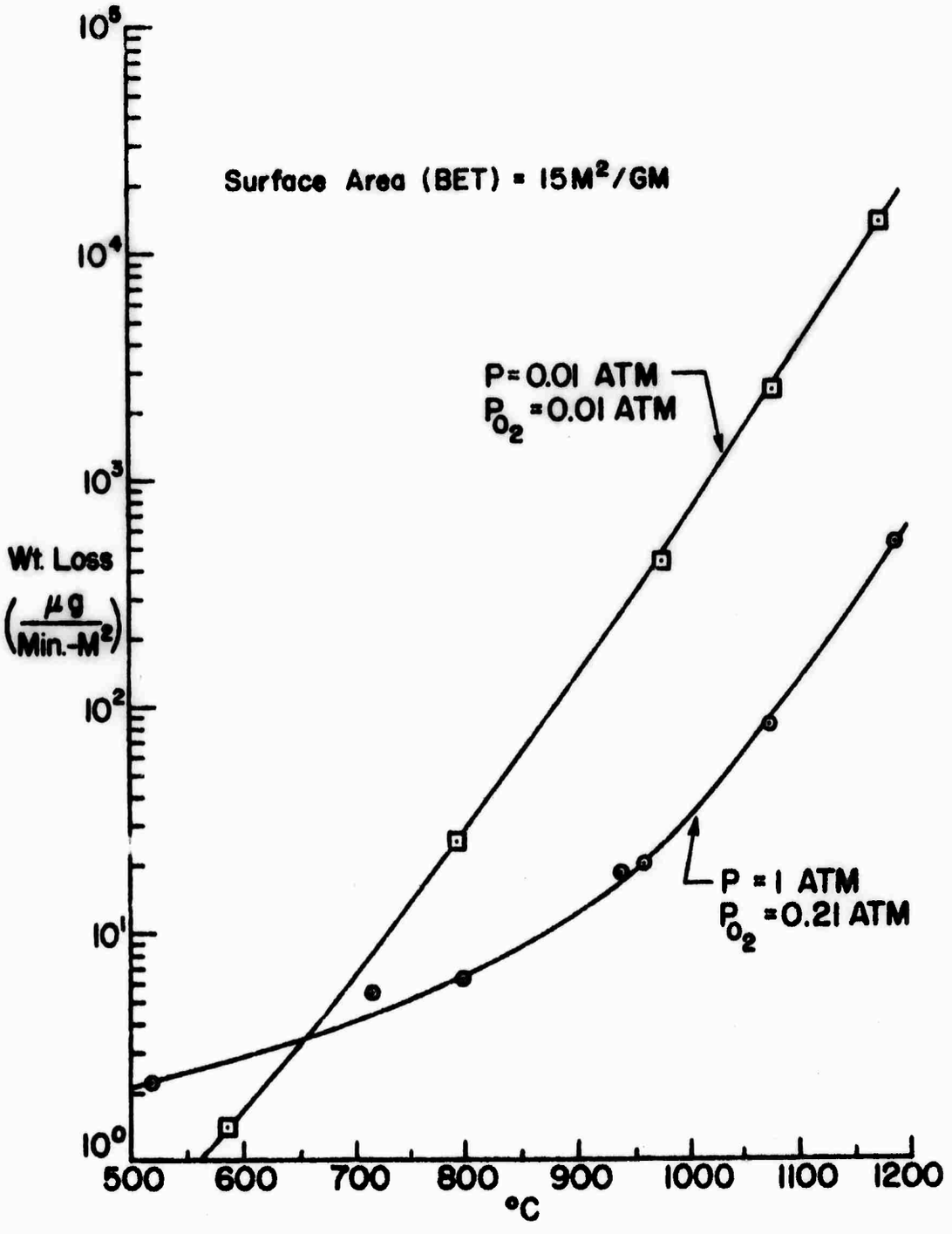

Figure 14. Vaporization of RuO_2

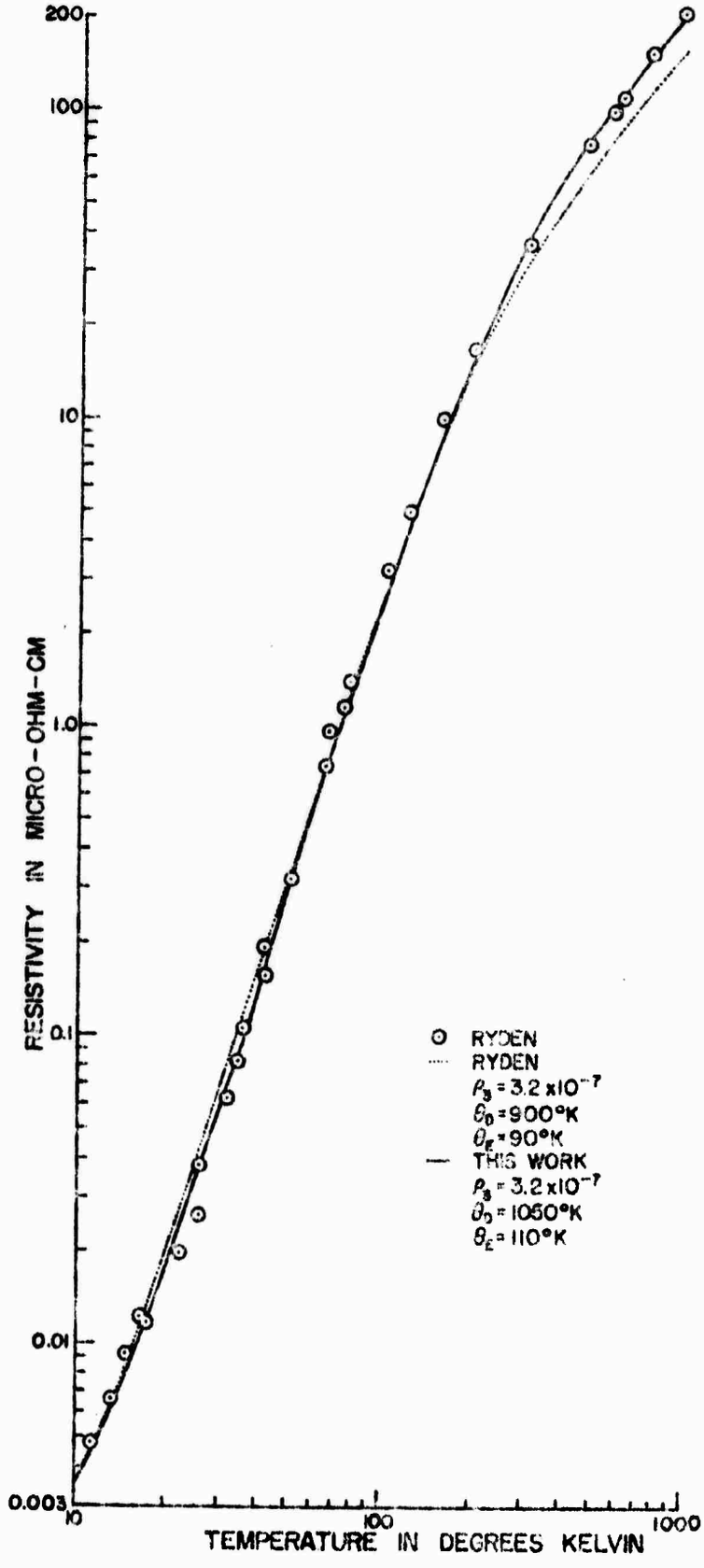

Figure 15. Defect-free Resistivity of RuO_2

As is shown in Fig. 15 discrepancies exist in two regions. The discrepancy in the region $10^{\circ}K$ to $40^{\circ}K$ is slight and is due to a simplifying assumption made in calculating the two terms of the equation. There does not seem to be a reasonable explanation for the discrepancy above $200^{\circ}C$.

Since the reported parameters do not work as well as indicated, a better fit was attempted. Simply increasing ρ_3 is not sufficient because it increases the discrepancy between $10^{\circ}K$ and $40^{\circ}K$; a value of ρ_3 that gives agreement at $300^{\circ}K$ is about 12% low at $T=1000^{\circ}K$. It is not possible to change ρ_2 because below $12^{\circ}K$ it is the only significant contribution to the resistivity. Therefore, only θ_D, θ_E, and ρ_3 can be varied. Values of $\theta_D = 1050^{\circ}K$, $\theta_E = 110^{\circ}K$ and $\rho_3 = 3.2 \times 10^{-9}$ $\mu\Omega$-cm/$^{\circ}K^2$ result in better agreement, as shown by the solid line in Fig. 15. The value of θ_D equal to $1050^{\circ}K$ disagrees with the Debye temperature of 610-670$^{\circ}K$ obtained from specific heat measurements [23]. However, it is common for resistivity Debye temperature to be larger than specific heat Debye temperatures so the discrepancy is not serious.

The band structure implied by the fit to Eq. (3) is partially substantiated by the deHass-van Alphen measurements of Marcus and Butler [22]. They report three values of effective mass for RuO_2: 0.51 m_e, 1.7 m_e, 3.5 m_e, where m_e is the rest mass of the electron. However, Ryden [21] argues that the band containing the 1.7 m_e electrons probably has a very low population whereas the other two bands are more heavily populated. Thus, the s band corresponds to the band with the .51 m_e electrons and the d band corresponds to the band with the 3.5 m_e electrons. The difference between the qualitative band structure [12] and that proposed by Ryden can now be understood. The qualitative model has one conduction band, which presumably would have a T^5 dependence at low temperatures and a T dependence at high temperatures, whereas the transition metal model requires two bands that can both be partially filled.

As part of this work the resistivity of a single crystal of RuO_2 was measured above room temperature. It had a diameter of about 70 microns and a distance between potential leads of about 1090 microns. All four leads were cemented in place with Englehard 6082 platinum paste. Fig. 16 shows the results, normalized at 200°C, obtained over several measurement cycles using the automatic resistance measuring system. The data show a decreasing slope for increasing temperatures resulting in a small curvature throughout the temperature range. The solid lines drawn through the data points are two straight line segments that approximate the curvature.

The two straight line segments are shown again in Fig. 17 for comparison with data by Osburn [24] and Ryden [21]. In order to compare defect free resistivities, the straight lines representing Fig. 16 have been modified assuming that the defect free resistivity would be 35.2 $\mu\Omega$-cm as reported by Ryden; a similar correction was made for Osburn's data. The dashed line on Fig. 17 is the calculated resistivity discussed earlier using the parameters obtained as part of this work.

Although Osburn's data are somewhat scattered, it agrees well with the results obtained in this work. Ryden's data are clearly different, having an increasing slope for increasing temperature. The calculated resistivity matching Ryden's data has an increasing slope because of the $\rho_2 T^2$ term, that is, because of the electron-electron scattering. A decreasing resistivity as observed here is not common among metallic conductors but the resistivity of platinum and palladium has a similar temperature dependence.

It should also be mentioned that the low temperature (<300°K) data of Ryden et.al. plus the high temperature resistivity data obtained as part of

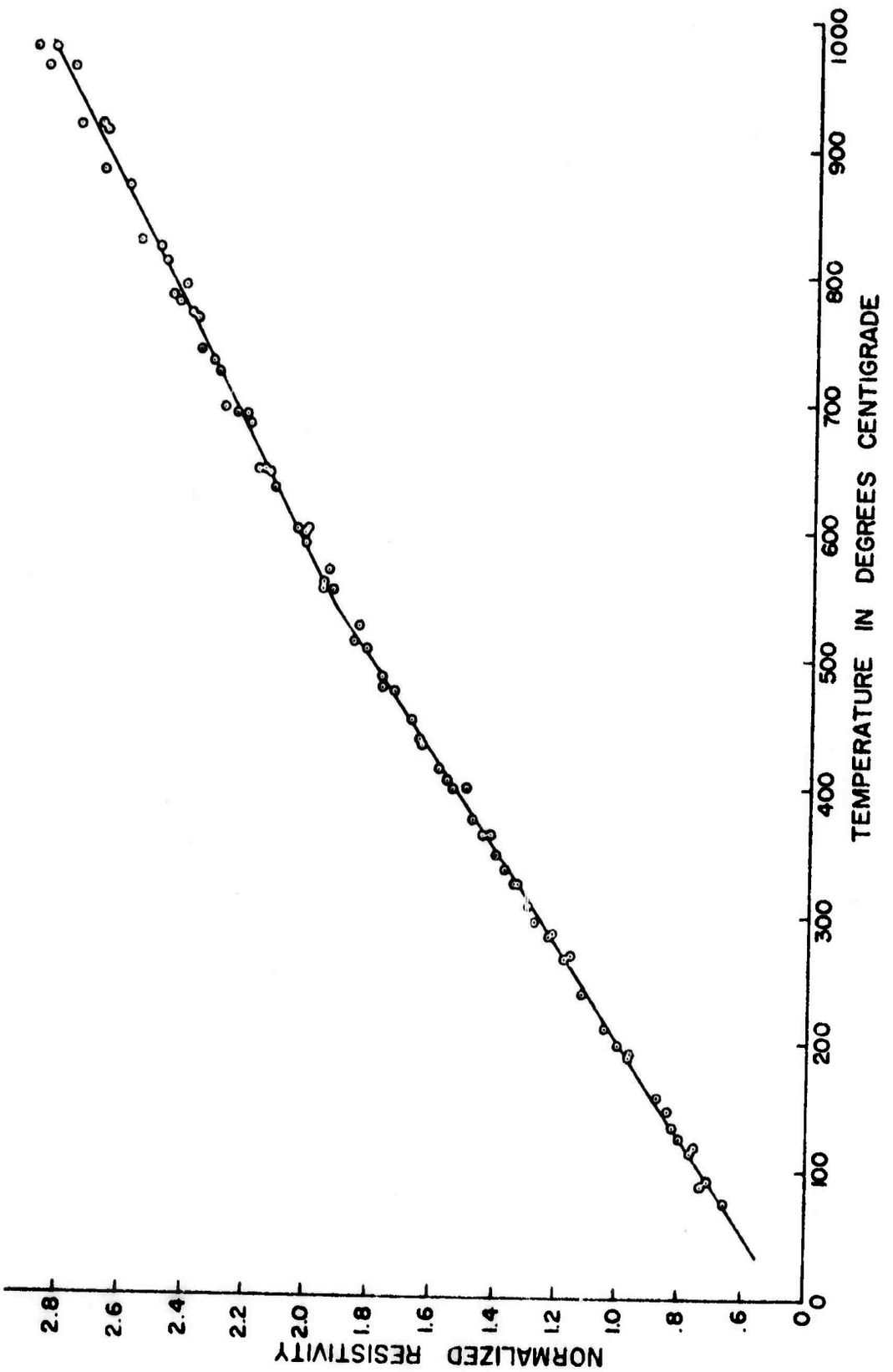

Figure 16. High Temperature Normalized Resistivity of RuO_2

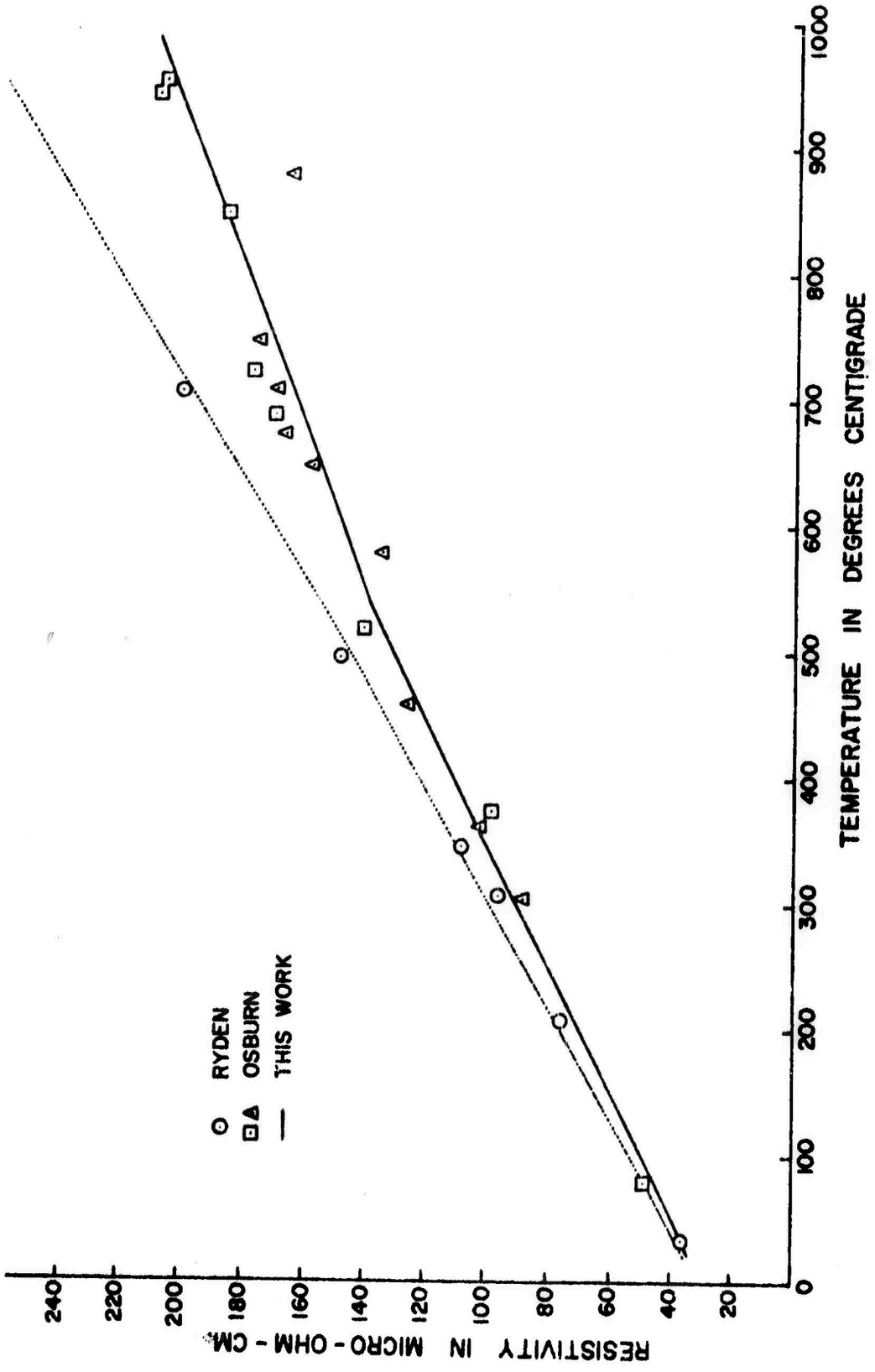

Figure 17. High Temperature Resistivity of RuO_2

this work can also be fit by including a non-trivial electron-phonon intraband scattering term. The fit is only good up to about 550°C where the decreasing slope causes a deviation. However, the curving high temperature resistivity as represented by the two straight line segments of Fig. 17 can be approximated well by having the value of the interband electron-phonon scattering term be constant. The significance of this would be that interband scattering becomes saturated and constant above 540°C leaving only intraband electron-phonon scattering and interband electron-electron scattering to be temperature dependent. A phenomena such as this might happen slowly resulting in curvature rather than an abrupt change in slope. Unfortunately, there is presently no theoretical support for such a model.

The conclusion that RuO_2 does not obey Mattheisson's rule was based on the resistivity measurements of just one crystal. Several other crystals with smaller residual resistance ratios were measured, and all obeyed Mattiesson's rule. The crystals measured in this study were also observed to obey Matthiesson's rule. Final resolution of this question must await a more quantitative description of scattering mechanisms in RuO_2.

The conclusion that RuO_2 has isotropic resistivity was based on a comparison of samples cut from platlet habits of RuO_2 crystals to the more common rod shape oriented along the c axis. The data points shown in Fig. 15 were obtained from both types of samples. This disagrees with the results of Fletcher, et.al., [11] who report anisotropy. They obtained resistivities in the 101 plane of 48.4 $\mu\Omega$-cm in the a direction and 67.9 $\mu\Omega$-cm in a direction at right angles. Several parameters, such as effective masses [25] of electrons have been found to be anisotropic so it would not be surprising if the resistivity was also anisotropic.

5. Intercomponent Effects

The relative values of the thermal coefficients of linear expansion of the glass, substrate, and RuO_2 are important in this material system because they

are the best indicator of strains that may be present. The fact that pressure dependent contact resistance has been proposed as an important mechanism determining resistor performance makes it more important than usual.

Fig. 18 shows the fractional elongation vs. temperature as reported separately earlier in this chapter. The values for RuO_2 are based on the volume expansion of the unit cell and represent, therefore, the average linear expansion of the RuO_2 powder. The agreement among the three elongations is very close. The best agreement is between the RuO_2 and the substrate, and if it can be argued that the more rigid substrate controls the elongation of the glass for relatively thin, thick film resistors, then the strain in the system should be very low. Even if this is not a valid assumption or if just glass and RuO_2 are used to make a pellet resistor, the change in strain with temperature should be very low in the temperature range between 150°C and the softening point of the glass where the two elongation curves are parallel. This similarity in fractional elongation casts doubt on the ability of a model based on pressure dependent contact resistances to explain all of the TCR effects of RuO_2 thick film resistors.

Other than for the papers dealing with thick film resistors, no information has been found discussing mixtures of the three basic ingredients used in this work. However, results have been reported for the system RuO_2 plus Na_2O-SiO_2 glasses. Three separate experiments have been reported: solubility of RuO_2 in glass, solubility dependence of ruthenium volatilisation from glass, and the oxidation state of ruthenium when dissolved in glass. These seem pertinent to this work and will be discussed briefly.

Wet chemical analysis was used to determine the solubility of the RuO_2 in glass. RuO_2 is insoluble in all acids so any RuO_2 not dissolved into the glass is insoluble. However, the ruthenium that has been dissolved in the glass is soluble, and $RuCl_3$ can be formed by dissolving the glass with an HF solution

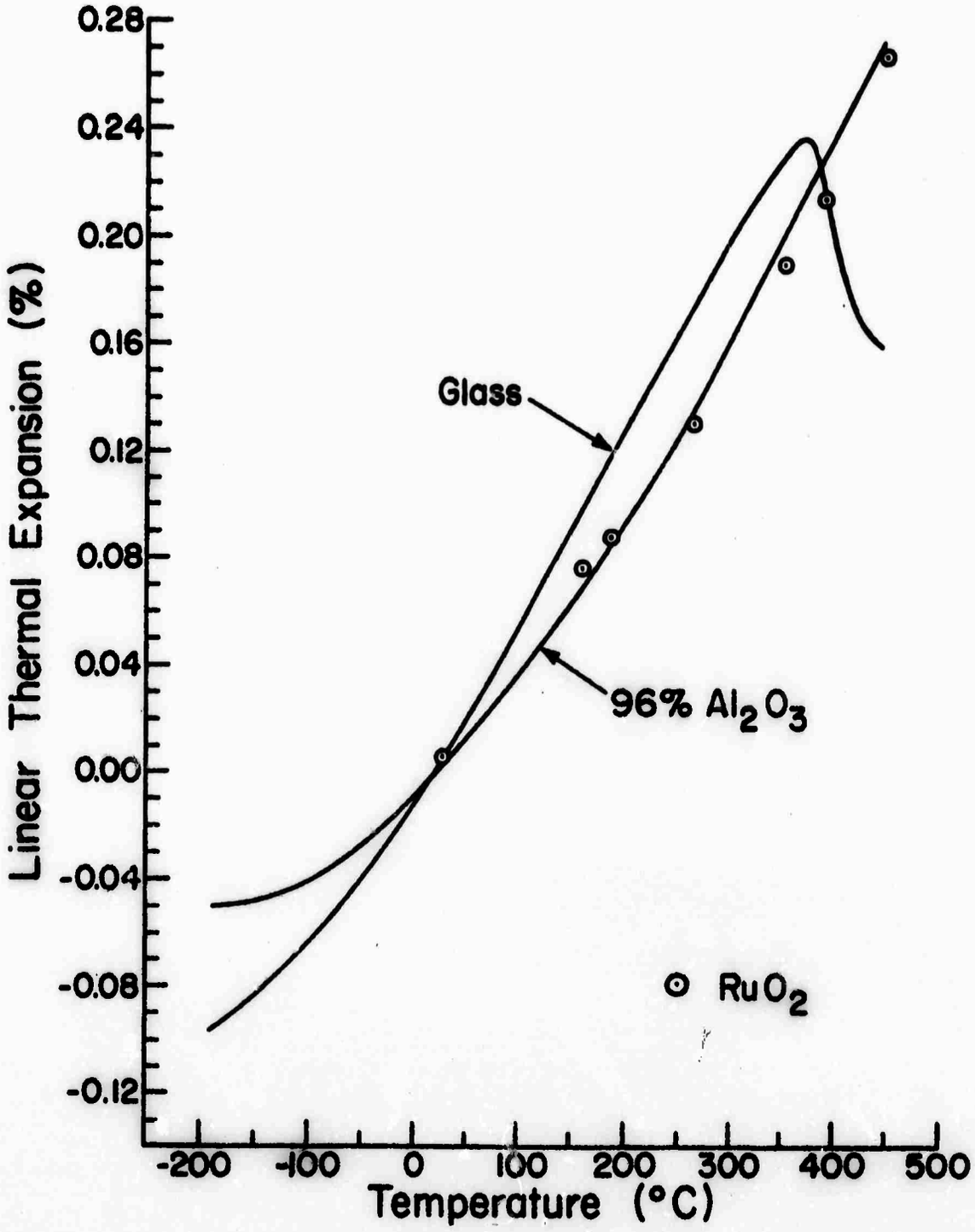

Figure 18. Thermal Expansion of Resistor Constituents

and treating the residue with HCl. The amount of $RuCl_3$ can then be determined. The solubility of RuO_2 in Na_2O-SiO_2 glasses was determined as a function of soda content and temperature [26]. The results show a rapidly increasing solubility for increasing soda content and an increasing solubility with increasing temperature, but the solubility is never great. Even for 1300°C and 40% Na_2O the solubility is less than 2200ppm, while for 20% Na_2O and 1000°C the solubility has decreased to less than 50 ppm.

The results of ruthenium evaporation from glass [27] can not be discussed quantitatively because of missing information. The conclusion is that below 40% Na_2O, the evaporation rate is proportional to the solubility of RuO_2 in glass when all other variables are constant. This is to be expected since the dissolved RuO_2 is the only source of ruthenium at the surface.

The most recent work in this RuO_2 - glass system is a determination of the valency of ruthenium as a function Na_2O content [28]. Calling low content Na_2O glasses acid and high Na_2O glasses basic, the authors conclude that tetravalent ruthenium exists in all glasses but that there is a tendency for trivalent ruthenium in acidic glasses and a tendency for hexavalent ruthenium in more basic glasses.

Na_2O creates more ionic-like bonds in glasses whereas the lead borosilicate glass selected for this work is probably more nearly co-valent. With this difference in microstructure it is difficult to apply the results discussed here to the lead borosilicate glass other than to extrapolate to low Na_2O content. This would imply that the solubility of ruthenium should be very low, perhaps only a few parts per million, that the evaporation of ruthenium from the surface of a thick film resistor would be very low at typical processing temperatures if all the ruthenium is dissolved, and that some dissolved ruthenium may be hexavalent instead of tetravalent as normally assumed.

B. Contact Resistance of RuO_2

Since one of the widely proposed models for the conduction mechanism in thick film resistors involves changes in contact resistance between adjacent conductive particles, it is important to determine the change in contact resistance with temperature and pressure in the absence of extraneous factors such as interactions between the conductive and the glass. To obtain the necessary data, the resistance of RuO_2 powder compacts was measured as a function of isostatic pressure at room temperature; later experiments will extend these measurements to different temperatures.

The samples were fabricated by isostatically pressing RuO_2 powder (0.05 μ^m average particle size) in a 3 mm diameter cylindrical rubber mold to 55,000 psi in order to develop sufficient green strength. Four, 0.13 mm diameter, platinum wires were wrapped around the sample along its axis to serve as current and potential leads, and the sample was encapsulated in a silicone rubber (General Electric RTV106). The sample was then placed in a high pressure cell fitted with electrical feed-throughs; the system utilized water as the working fluid.

The resistivity as a function of pressure is shown in Fig. 19 for four compressions and decompressions. The magnitude of the resistivity of the powdered compact is two orders of magnitude greater than that of single crystal RuO_2 (see Fig. 17), so it is reasonable to assume that the measured value consists solely of contact resistance. A maximum pressure of 15,000 psi was chosen because residual stresses greater than this could not be tolerated in a thick film resistor without causing fracture.

It is significant to note that the total contact resistance changed only by a factor of two over the pressure range 0-15,000 psi. This result means that changes in pressure on the contact between adjacent conductive grains due to mismatch of thermal expansion among system components is insufficient in itself

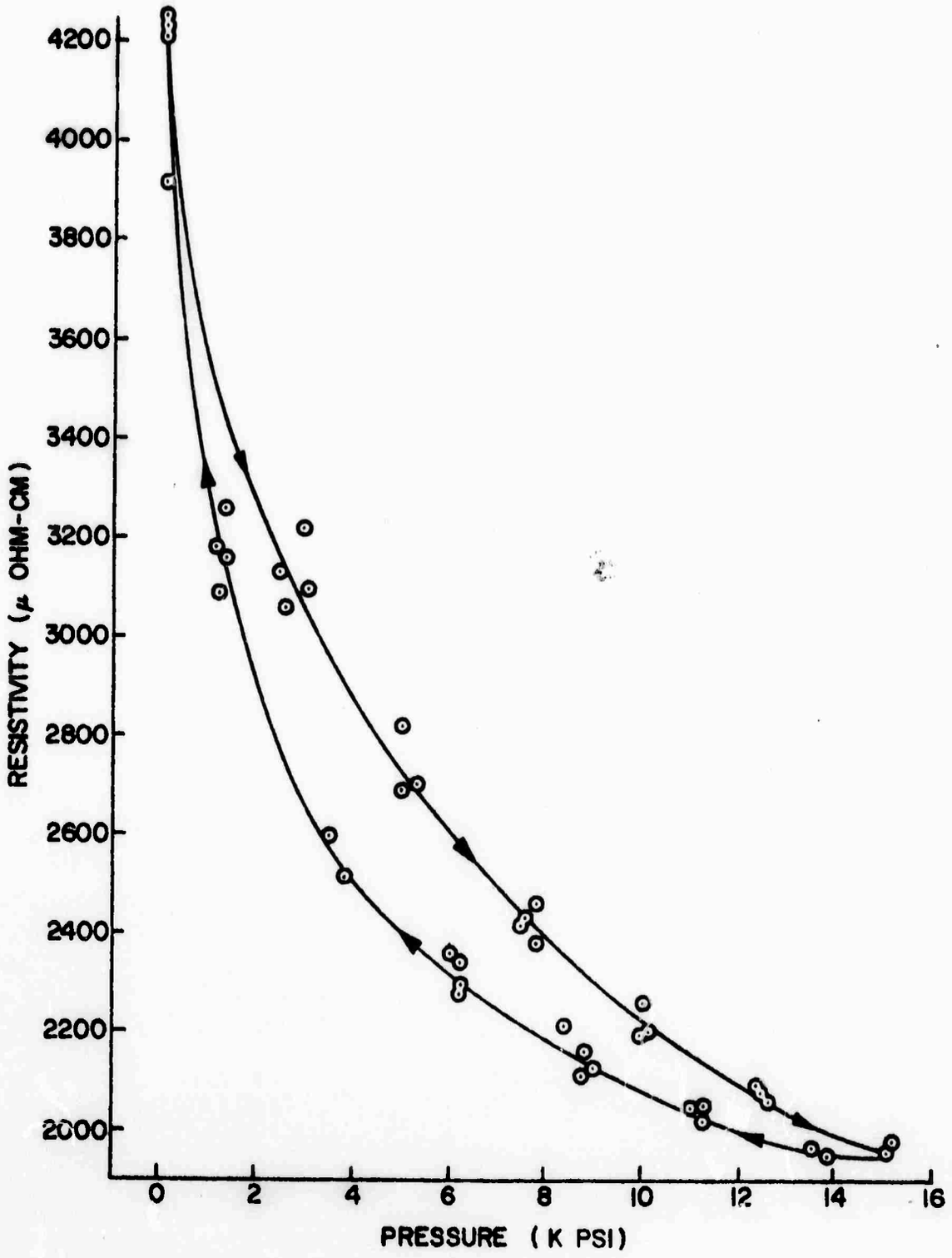

Figure 19. Isostatic Pressure Dependence of the Resistivity of RuO_2 Powder Compact

to compensate for the change in resistance with temperature of the RuO_2 grains. The contact resistance model may still have merit if the temperature coefficient of contact resistance is found to be large and negative, or if one assumes that the measured resistance in a thick film resistor is completely due to contact resistance between grains. Both of these possibilities will be explored.

C. Single Crystal RuO_2 in Glass

Steady-state data, either resistance vs. time or resistance vs. temperature could not be obtained with the desired repeatibility at high temperatures. This was due to the wetting characteristics of the glass coupled with its low viscosity at high temperatures. The glass would "creep" out of the recess and across the surface thereby decreasing the amount between the measurement electrodes. In addition, the motion of the glass would produce strains on the RuO_2 crystals which eventually led to fracture in all cases. Therefore, the results presented are essentially kinetic data, and as such can give only a qualatative picture of the RuO_2-glass interaction.

Measurements consisting of sample resistance as a function of time and temperature were obtained for four small crystals. For each sample, a table is included that summerizes the temperature vs. time history of each sample and a graph of sample resistance vs. temperature recorded at different points in the history of the sample is presented. Almost all heating and cocling rates were 30°C/minute.

Table VIII and Fig. 20 show the behavior of Sample 11. Cycle 072170A is the first exposure of the crystal to high temperature and glass, and the sample resistance decreases at high temperature to a value substantially below that for single crystal RuO_2. On the cooling portion of this cycle the high temperature resistance is higher. With repeated exposures to near 900°C for varying lengths of time, the decrease in resistance is still apparent but the temperature at which it begins is higher. The resistance vs. temperature seems

Table VIII. Thermal History of Sample 11 (RuO_2 single crystal 1.98 μm diameter)

Measurement Cycle	Max. Temp. (°C)	Time at Max. Temp. (Minutes)
072170A	880	.5
072170B	930	8
072170C	925	20
072270A	950	44
072470A	802	Sample broke

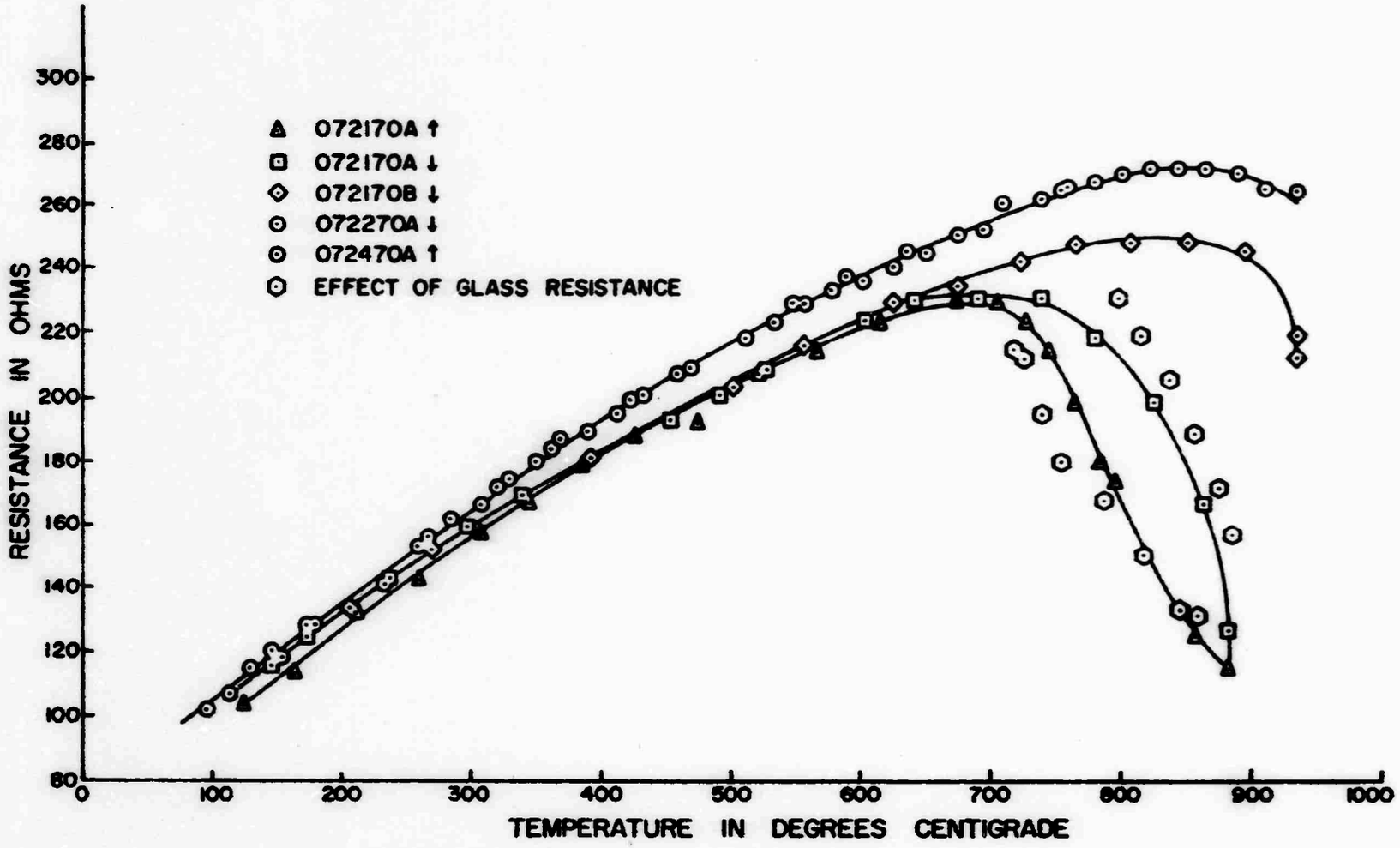

Figure 20. Temperature and Thermal History Dependence of the Resistance of Sample 11

to reach an equilibrium condition after a sufficient exposure to high temperature. For this sample, the maximum resistance for the equilibrium condition occurs at 870°C. Fig. 20 also seems to show a small monotonic increase in the sample resistance for all temperatures. However, this trend could be mostly due to uncertainties in the measurement system. Counter examples are shown later.

Table IX gives the history of Sample 16 and Fig. 21 shows resistance vs. temperature at different points in the sample history. Measurement cycle 092870D was the first high temperature exposure with glass and a decrease in resistance is observed. This cycle had a minimum duration at 900°C (.5 minute), and was followed by an identical cycle. The third measurement cycle (092970B) was again to 900°C but had a high temperature duration of about 6 minutes. From the increasing portion of 092970B it can be seen that the previous two brief exposures to 900°C did not cause a significant effect as it did for Sample 11. However, the effect of the 6 minutes at 900°C can be seen. There is a permanent increase in the high temperature resistance.

Sample 19 was the first small crystal to use a lid over the well in the substrate to retard the flow of glass out of the well onto the substrate surface. This feature at least aided in maintaining a longer life for the sample, thereby permitting resistance vs. time measurements at high temperatures. Also, the resistance at 70°C was measured between almost every measurement cycle in an attempt to determine the amount of the crystal that dissolved into the glass, or to serve as an indicator of possible new phases that might form. These measurements were hindered by the lead wires separating from the crystal; the initial measurements were made with four lead wires to the crystal, but after several cycles only two remained. This makes it impossible to directly compare the resistance continuously throughout the life of the sample.

Table X summarizes the history of Sample 19, and included the resistance values measured at 70°C with a high accuracy D.C. system. Fig. 22 shows the

Table IX. Thermal History of Sample 16 (RuO_2 single crystal 1.79 μm diameter)

Measurement Cycle	Maximum Temperature (°C)	Time at Max. Temperature (Minutes)	Comment
092870C	691	.5	Included because the glass was in contact with the crystal at the end of the cycle although no change could be seen in the resistance
092870D	892	.5	
092970A	892	.5	
092970B	915	6	As can be seen on Fig. 21 the 6 minutes at high temperature caused a permanent change in the high temperature resistance
100170A			Attempted DC resistance measurements. They indicated slowly increasing resistance while the AC resistance measurements indicated decreasing or constant resistance.

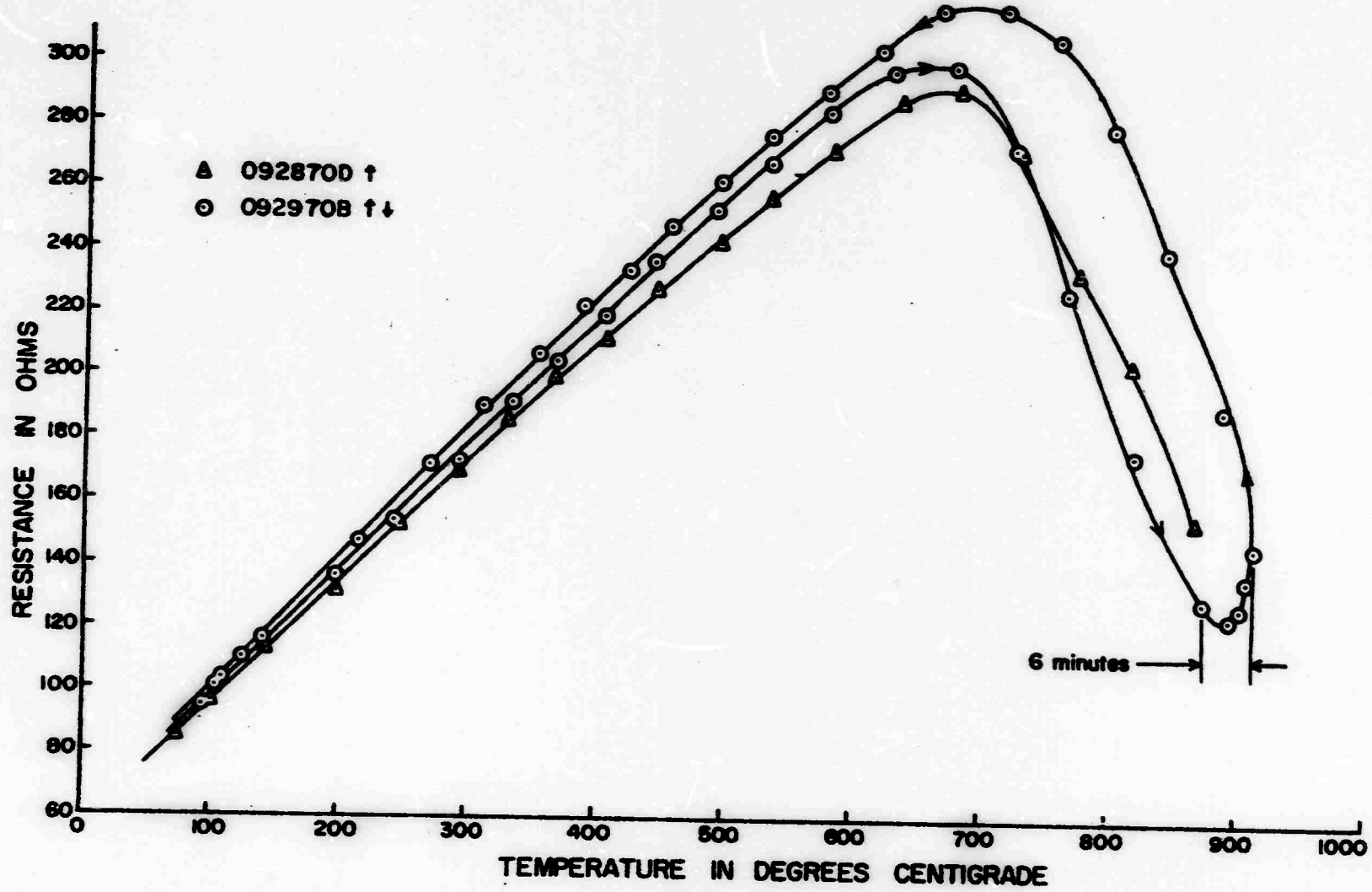

Figure 21. Temperature and Thermal History Dependence of the Resistance of Sample 16

Table X. Thermal History of Sample 19 (RuO_2 single cyrstal 2.11 μm diameter)

Measurement Cycle	Maximum Temperature (°C)	Time at Max. Temperature (Minutes)	Sample Resistance at 70°C (Ohms)	Comments
			65.763	
112570B	774	.5		Glass was in contact with all of the crystal and covered half the crystal.
			67.670	
112770A	831	.5		A decrease in high temperature resistance was observed.
			133.43*	
112770B	687	.5		Prior to the beginning of this cycle a lead wire to the crystal became open. This caused a new sample resistance. Add glass.
			132.08	
120270A	687	.5		Add glass. After this cycle another lead became loose from the crystal. The configuration is now four leads to the substrate but two leads on the crystal.
			132.60*	
120370A	665	.5		Add glass. Placed a lid over the well to slow the rate of glass migration.
			133.27	
120370B	871	.5		Heated slowly to 900°C the cooled rapidly.
			130.52	
120370C	842	.5		Heated rapidly to 900°C then cooled slowly.
			127.57	
120670A	868	,5		Heated and cooled rapidly.
			129.30	
120670B	795	80		Held at 800°C and attempted to measure resistance versus time. No change was observed.
			128.24	
120770A	795	184		Repeat 120670B. No change in resistance was observed.
			126.85	
120870A	775	.5		
120870B	795	204		Repeat 120670B. No change in resistance was observed.
			126.14	
120970A	867	.5		

Continued

Measurement Cycle	Maximum Temperature (°C)	Time at Max. Temperature (Minutes)	Sample Resistance at 70°C (Ohms)	Comments
			126.12	
120970B	977	.5		Measure to 1000°C.
			123.64	
120970C	967	.5		Measure to 1000°C.
			122.40	
121070A	970	40		Resistance increased during this interval, then failed by breaking.

*Lead wire configuration changed

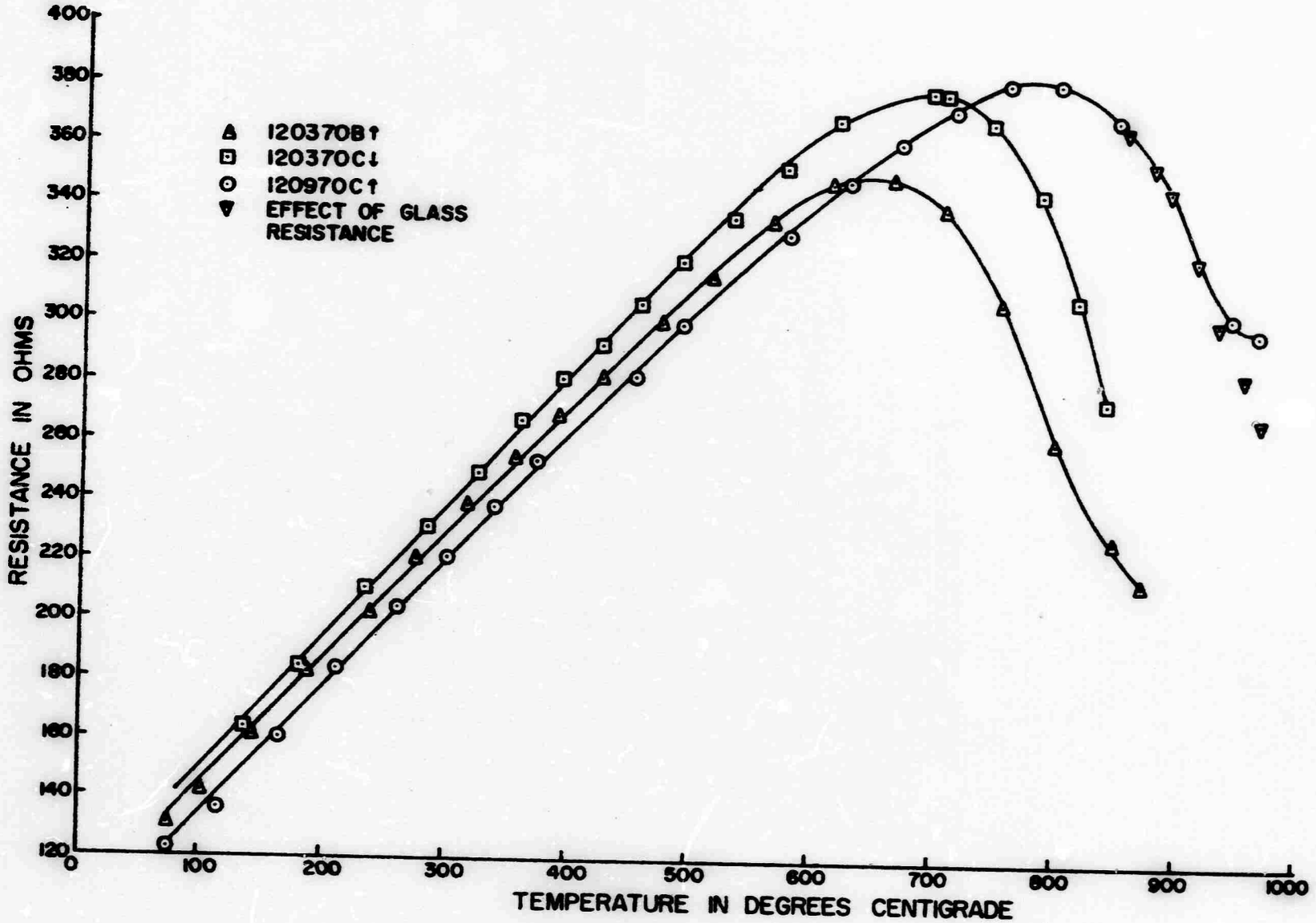

Figure 22. Temperature and Thermal History Dependence of the Resistance of Sample 19

resistance vs. temperature at various points in the history of the sample as indicated. The results depicted in Fig. 22 show that Sample 19 had the same basic behavior as the earlier two samples, but the increased number of cycles permits additional insight. The resistance measurements at 70°C indicate an increase of 2.9% during the first exposure to glass and high temperature. If this is not due to the changes in lead wire geometry that occur during glass encapsulation, it would indicate slight solubility of RuO_2 in the glass. After this initial increase, the resistance remains constant and then decreases about 8% during the last 2/3 of the sample life. Other than this decrease, the room temperature sample resistance remained constant throughout all measurement cycles and in particular it did not increase during a total of 7.8 hours at 800°C.

Sample 21 was prepared primarily to investigate more thoroughly the initial formation of the decreased resistance at high temperature. Using the technique mentioned earlier, the well was filled with glass so that the glass covered the platinum conductive paths but did not contact the crystal or lead wires. Then the sample was heated to 800°C, cooled to about 370°C, and then recycled to 800°C, all at 120C°/min. Figure 23 shows the resistance vs. temperature of the sample. As can be seen, the resistance begins to decrease at about 640°C in a manner similar to the previous three samples on initial heating as well as on a repeated cycle. This is important because all previous observations indicate that the glass could not have made contact with the crystals at temperatures below 700°C, particularly with the rapid heating rate.

Table XI summarizes the brief history of Sample 21, and shows the resistance at 70°C before and after the first high temperature exposure to glass. The sample resistance was increasing during a measurement of resistance versus time at 900°C when the crystal broke. Several minutes after the crystal broke the sample resistance was equal about 1000 ohms; this value of resistance in parallel with the crystal

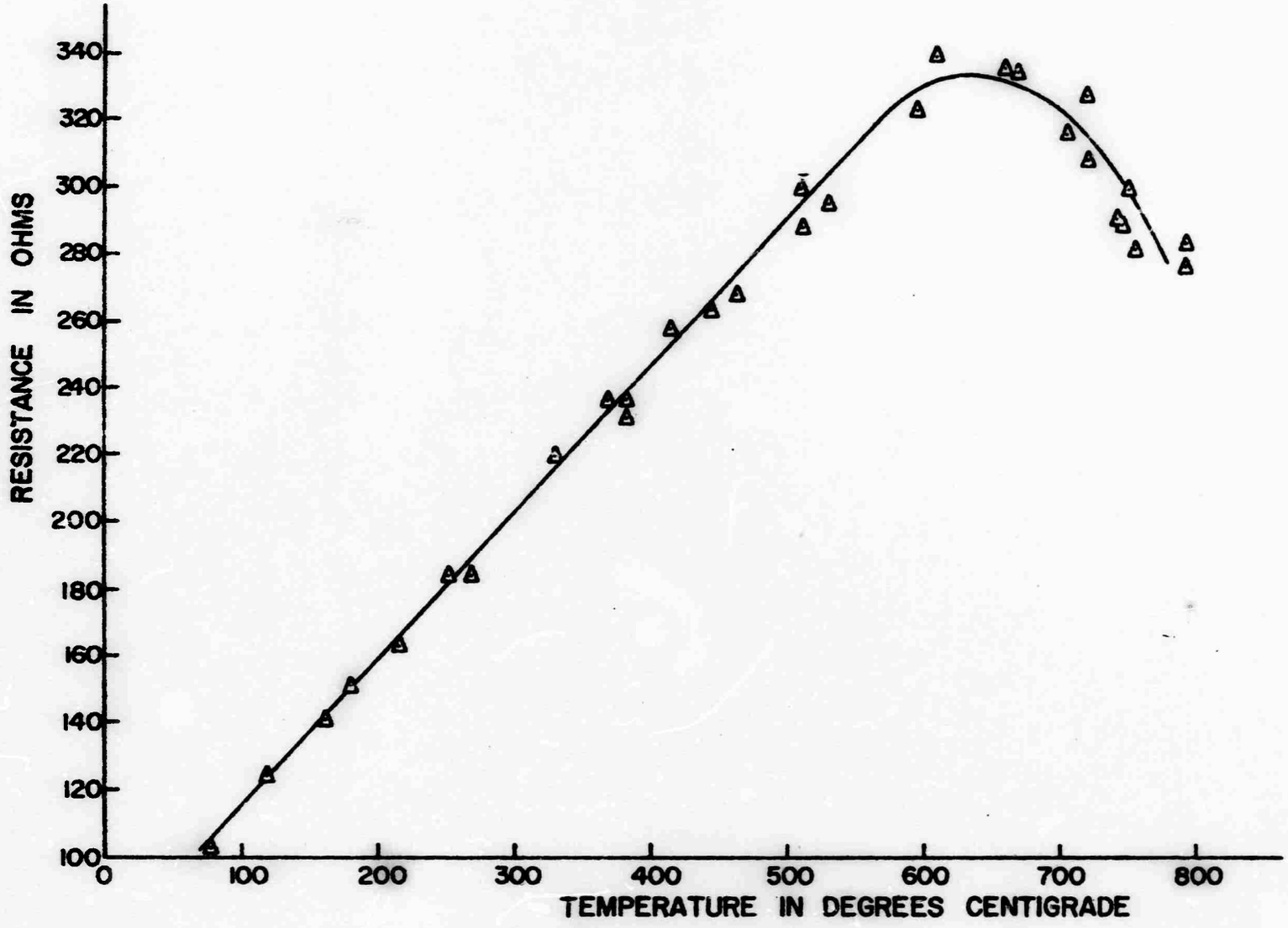

Figure 23. Temperature Dependence of the Resistance of Sample 21

Table XI. Thermal History of Sample 21 (RuO_2 single crystal 2.10 μm diameter)

Measurement Cycle	Maximum Temperature (^{o}C)	Time at Max. Temperature (Minutes)	Resistance at 70^{o}C (ohms)	Comments
			93.99	
010870C	790	.5		Two cycles to 800^{o}C at 120^{o}C/min. heating and cooling
011170A,B,C	700	.5		Add glass and attach lid
			95.06	
011270A	900			Sample broke after 30 minutes. The higher resistance after breakage was the value necessary to explain the decreased resistance at 900^{o}C

resistance was equal to the value of the sample resistance before the crystal broke.

The resistivity of glasses decreases with increasing temperatures with an activation energy that is typically about 1 ev. To determine the contribution of the glass resistance to the behavior of the small crystal samples, two experiments were conducted. First, Sample 19, with the broken crystal, was remounted in the furnace for resistance versus temperature measurements. Fig. 24 shows the results of this measurement. The logarithm of the sample resistance is plotted versus reciprocal absolute temperature, and shows that the resistance was slightly higher during the decreasing temperature portion of the cycle. Visual observation at the completion of the cycle indicated that the crystal sections has separated substantially. The increased resistance was at least in part caused by this process.

To further investigate the influence of the glass in high temperature resistance measurements, a substrate was prepared with electrode geometry similar to that used for the crystals, but without a crystal (Sample 24). As with the small crystal samples, glass was added and fired to 700°C until the well was reasonably filled. A lid was then placed over the well and the sample heated to 800°C. At near maximum temperature the resistance measuring system was connected and the resistance was measured as the sample cooled to give the results shown in Fig. 24. The sample was then heated to 900°C and maintained there for 11 minutes, which resulted in a permanent increase in the resistance for all temperatures. The well was then refilled with glass powder and the sample was reheated to 900°C for a short time. The resistance began at a lower value but after exposure to 900°C, increased to nearly that of the previous measurement cycle (see Fig. 24).

The most obvious effect observed in experiments with small crystals encapsulated in glass is the decrease in resistance at high temperatures.

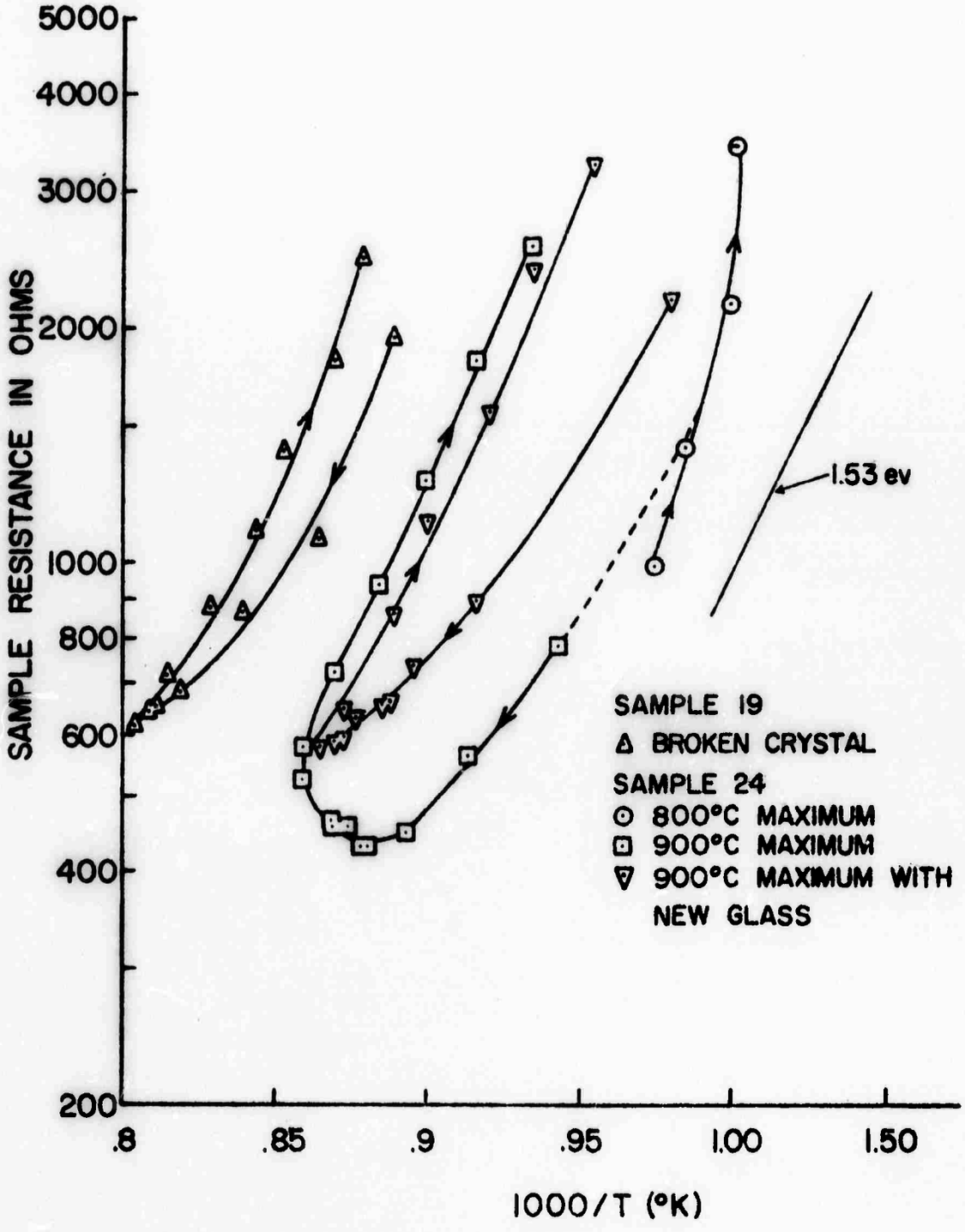

Figure 24. Temperature Dependence of the Glass Resistance

There seems to be more than ample evidence that this phenomena is related to the conductance of the glass. One example is the ability to correlate the resistance versus temperature of Sample 24, using only glass and no crystal, to the behavior of Sample 11 as shown in Fig. 20. The procedure was to adjust the resistance versus temperature of Sample 24 measured early in the exposure to high temperature so that the crystal resistance in parallel with the glass resistance agreed with the resistance versus temperature measured in the initial cycle of Sample 11. This adjustment was done by multiplying all resistance values by a constant to compensate for different geometries. The resistance values of Sample 24 measured after 11 minutes at 900°C were adjusted by the same constant and the parallel combination was again calculated. The results of this calculation are also shown in Fig. 20. As can be seen, the calculations predict the same drift with temperature as was experienced with Sample 11.

The resistance versus temperature of Sample 19 after the crystal broke more directly yields the same result. Sample resistance was calculated using the resistance of the RuO_2 crystal and the glass resistance reported in Fig. 24 obtained during the cooling portion of the measurement cycle when the ends of the crystal were farther apart. The calculated values plotted in Fig. 22 show excellent agreement with sample behavior prior to the crystal breaking.

The third observation that supports the claim that the decrease in resistance at high temperature is due to the glass is the behavior of Sample 21. As mentioned earlier, the decrease in resistance shown in Fig. 23 could not be due to an interaction between the small crystal of RuO_2 and glass, such as the formation of a new phase, because the glass would have not been in contact with the crystal during the initial period of high temperature. Since the glass was in contact with the conductive paths leading to the crystal there could be a condution path through the glass, however.

The activation energy for conduction in the glass can be determined from the slope of the lines in Fig. 24. A line has been drawn parallel to the experimental curves corresponding to an activation energy of 1.53 ev.

The reason for the resistance of the glass to increase with time at high temperatures is not known. One possibility is that because the glass leaves the sample well and creeps out on to the alumina surface, the increase in resistance would be due to less glass, i.e., the resistivity of the glass would remain constant and the resistance change would be due to a geometry factor. The fact that the resistance approaches an equilibrium condition could be due to the surface diffusion decreasing as the surface is covered. However, some of the small crystal samples, particularly Sample 19, went various lengths of time with and without additions of glass, and the behavior at high temperature remained about the same. Sample 24, without a crystal, shows a similar effect. During the 11 minutes at high temperature the resistance measured at 810°C increased by a factor of 3.5; it is doubtful that the amount of glass in the vicinity of the electrodes decreased by a factor of three, but it is difficult to estimate the changes in geometry factor of the glass, particularly when a lid is in place. When more glass was added the resistance began lower but gradually increased to near the original value.

The lower resistance before exposure to high temperature could also be due to a low resistivity of the glass that begins to increase at higher temperatures. There should be a greater defect concentration in the glass early in its thermal history; in particular there may be some metallic lead present. This would change the concentration of charge carriers as measured at 1000 Hertz and would decrease with time at high temperatures. However, such conduction mechanisms would usually have different temperature dependencies than the more defect-free material. More careful resistivity measurements

in which the geometry will not change will be required to resolve this point.

As was predicted earlier from the low temperature, low Na_2O, extrapolation of the results of Mukerji and Biswas [26], the solubility of RuO_2 in glass is apparently very low. The results of prolonged exposure to 800°C for Sample 19 failed to produce any significant increase in resistance as measured at 70°C. In fact, during this time the sample resistance decrease slightly. For the case in which solubility is very low, there is usually a rapid initial diffusion due to the high concentration gradient. Then, as the host material becomes saturated the concentration gradient decreases and diffusion decreases. In an effort to observe this initial diffusion, the resistance of two crystals was measured before and after initial glass encapsulation. Sample 19 increased by 3% and Sample 21 increased by 1%. To quantitatively determine the solubility and diffusion of RuO_2 into the glass it will be necessary to do direct analysis with electron microprobe.

The reason for the decrease in the resistance of Sample 19 during the last half of its life is not known. It could be due to the formation of a new low resistivity phase near the RuO_2 crystal, but there is presently no conclusive evidence that such a material exists. The change could be due to the glass ingredients changing the resistivity of the RuO_2, but impurities would more likely increase its resistivity. The platinum paste could also be sliding along the length of the crystal to form a smaller length dimension, but this also seems unlikely.

In summary, the series of experiments performed with small crystals failed to clearly detect the formation of any phase other than the RuO_2 single crystal and glass, although effects were observed that could be explained by the existance of a new low resistivity phase, probably containing ruthenium. The solubility of RuO_2 in the lead borosilicate glass is low and the diffusion

of RuO_2 is insignificant over large distances although for sufficiently short distances it may be significant. The glass was shown to have a relatively low resistivity at high temperatures that may increase by a factor of about 3-5 with sufficient exposure to 900°C or above. The reason for this latter phenomena is not known.

D. Resistors

For the initial studies of thick film resistors it was considered essential to eliminate as many as possible of the variables that normally accompany resistor processing. The approach chosen was to employ an alumina substrate on which the fired platinum conductive had been carried down into a recessed area in the center of the substrate. This was similar to the substrates utilized for mounting the small RuO_2 single crystals, but without the crystal mounting wires (see Fig. 8a). The resistor "formulation" consisted of only 3% by weight RuO_2 powder (BET surface area = 15 m^2/gm which calculates to an average particle size of 0.05 μm) and glass powder (BET surface area = 1.25 m^2/gm which calculates to an average particle size of 1.03μm). The two powders were mechanically mixed, and then ground in an alumina morter and pestile for 15 minutes. The recessed area in the substrate was then filled with this powder.

The room temperature resistance with only the powder in the recessed area was $>10^7$ ohms. The resistor was then fired and the resistance recorded continuously; the results of this experiment are shown in Fig. 25. The profile was a linear rise of 30°C/min. to a maximum temperature of 900°C followed by a linear cooling at the same rate. The resistance remained very high until a temperature of approximately 750°C was reached at which point it dropped very rapidly, reached a minimum at the maximum temperature, increased as the temperature decreased, reached a maximum at 575°C, decreased until the

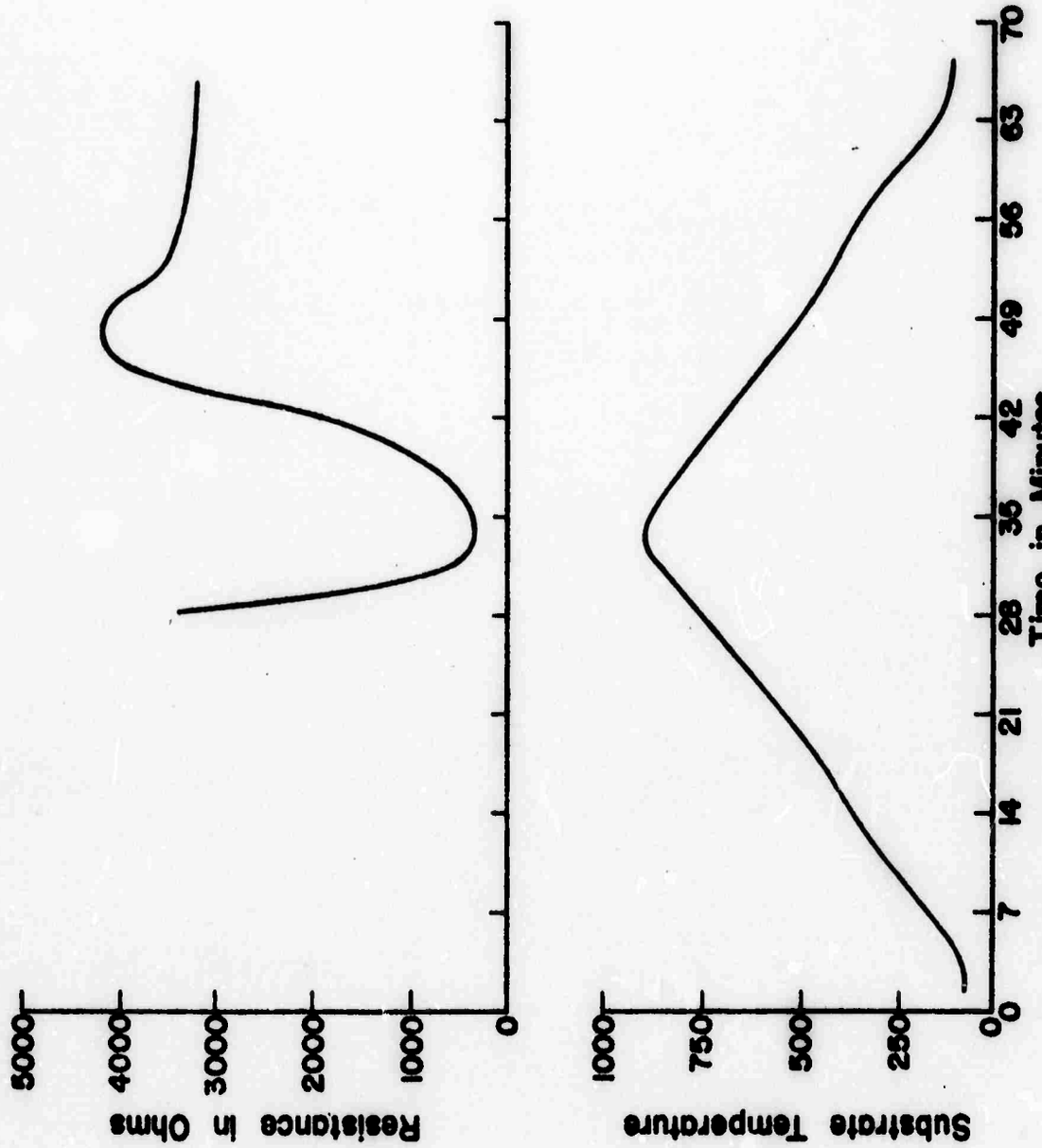

Figure 25. Formation of an RuO_2 Resistor

temperature reached approximately 450°C, and then remained nearly constant to lower temperatures. Remeasuring the temperature dependence of resistance for this resistor gave the results shown in Fig. 26. Again, the resistor shows a very small temperature dependence up to 450°C at which point the resistance increases rapidly, goes through a maximum near 575°C, and then decreases rapidly with further increases in temperature. The resistance of single crystal RuO_2, normalized to the resistor resistance at room temperature, is also plotted for reference on Fig. 26.

The behavior of the resistor above the softening point of the glass (480°C) is very similar to the behavior of the small RuO_2 single crystals in glass (see Fig. 20-23). The temperature dependence of the resistance from 450° to 500° is the same as that for single crystal RuO_2 (compare with the slope of the dashed line on Fig. 26), and the high temperature behavior can again be correlated with the glass conductance. Thus, it appears that at temperatures above the softening point of the glass, the TCR of an RuO_2 resistor is determined by the TCR of RuO_2, and there is no "TCR anomaly".

At the softening point of the glass there appears to be an abrupt change in conduction mechanism. An elucidation of the nature of this low temperature conduction mechanism is one of the primary goals of the project, and the knowledge that conducting paths having the same TCR as the conducting phase are present above the softening point of the glass is a valuable new fact which must be accounted for by any comprehensive model.

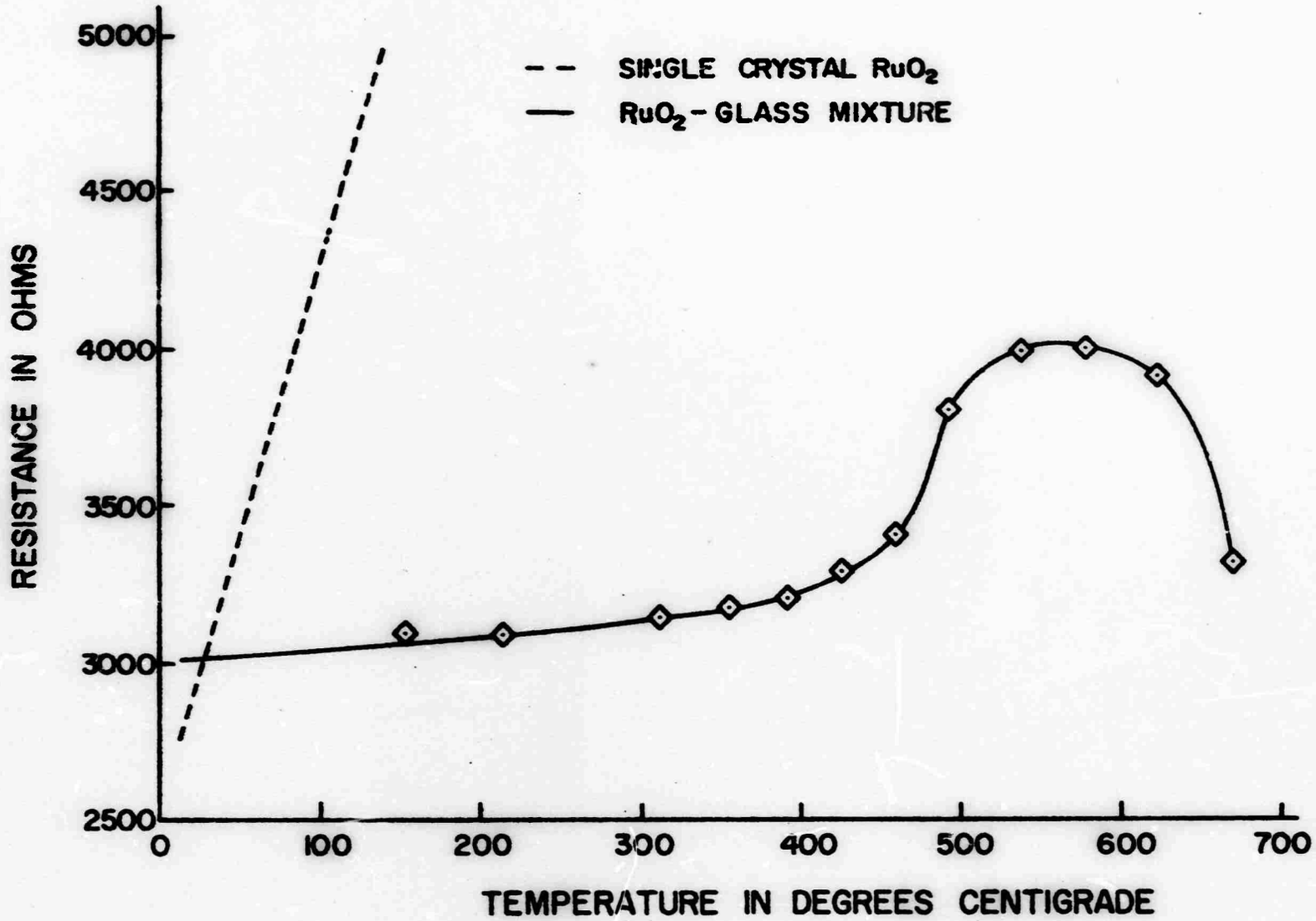

Figure 26. Temperature Dependence of the Resistance of an RuO_2 Resistor

IV. Summary and Future Plans

It was recognized at the initiation of this project that elucidation of the conduction mechanisms in thick film microcircuits was a complex problem; the results presented in this report further substantiate this fact. In order to accomplish the goals of this project it is necessary to keep the test system as simple as possible, and this has been accomplished. It was demonstrated that a resistor having the essential characteristics of commercial thick film resistors can be fabricated from the test system, RuO_2-glass-substrate, with no additional ingredients (e.g. no organic screening agent). The intrinsic properties of the test system ingredients have been satisfactorily established, and results on some inter-component effects have been obtained. Based on the results to date, limits can be placed on the contributions of various effects. In particular, the contact resistance model must be re-examined in light of the small change in contact resistance observed as a function of isostatic pressure, and the fact that a low TCR resistor can be made from constituents having very closely matched thermal expansions. The low solubility of RuO_2 in the glass, and the absence of rapid interactions between the two pose a serious question concerning the validity of the degenerate semiconductor glass model; the observations reported here indicate that incorporation of sufficient RuO_2 to form a degenerate semiconductor during the time-temperature conditions employed in resistor processing is unlikely. In addition, the results to data more clearly define the important areas for future work.

Work directed toward resolving the "TCR Anomaly" and developing models for conduction mechanisms in thick film resistors will continue.

In order to establish the influence of thermal stresses:

1. Measurements of the contact resistance of RuO_2 powder as a function of both temperature and pressure will be completed.

2. The coefficient of thermal expansion of the glass will be varied by changing the ratios $PbO/B_2O_3/SiO_2$, and the effect on resistivity and TCR of massive glass-RuO_2 samples determined.
3. Substrates with coefficients of thermal expansion differing by more than a factor of ten have been obtained and flame sprayed with a thin coating of alumina so that the resistor - substrate interface will be the same in all cases. The resistance and TCR of resistors printed and fired on these substrates will be measured.

In order to establish the influence of new phases:

1. The diffusion of RuO_2 into the glass will be measured with the electron microprobe.
2. The electrical properties of the contact region between two crossed single crystals will be studied.
3. Measurements of resistivity as a function of time will be made on the small crystals encased in glass. These data when combined with the diffusion results will permit estimates of the electrical properties of the new phases formed.

In order to determine particle size effects, it will be necessary to develop procedures for determining particle size distributions in the starting material and in the fired films. Since the size range of interest is sub-micron, this work must await installation of the scanning electron microscope (estimated April, 1971).

Studies of resistor and conductor microstructure as a function of material properties and processing conditions will be initiated. This work also requires the scanning electron microscope. The kinetics of microstructure formation during resistor firing will be studied in a high temperature X-ray diffractometer.

Studies of thick film conductives using Pd, Ag, Pt and Au will be initiated. The mutual solid solubility exhibited by several of the binary alloys will

enable the study of composition effects while holding either resistivity or TCR constant. Electrical properties, coefficients of thermal expansion, diffusivities, and various thermodynamic properties have been thoroughly studied in most of these systems. The significant thick film properties in this investigation are electrical properties, compatibility and solderability, adherence to the substrate, thermal expansion and stress distribution, and sensitivity to migration.

Studies will be initiated in the areas of formulation rheology and screen printing. The purpose of these studies will be to reduce the variations in resistor properties due to these two factors to a small and known level.

V. References

1. B. S. Verma and S. K. Sharma, Thin Solid Films, 5, R44(1970).

2. L. J. Brady, IEEE Electronic Components Conference, 238(1967).

3. C. J. Pukaite and G. Goodman, Bull. Am. Cer. Soc., 48, 428(1969)(Abstract) Presented at the Annual Meeting, Am. Cer. Soc. May 1969.

4. F. M. Collins, Bull. Am. Cer. Soc., 48, 805(1969)(Abstract) Presented at the Fall Meeting of the Elec. Div. of the Am. Cer. Soc. Sept. 1969.

5. L. C. Hoffman, Bull. Am. Cer. Soc., 42 490(1963).

6. E. H. Melan and A. H. Mones, IEEE Electronics Components Conference p. 76(1964).

7. G. S. Iles, IERE Conference Proceedings 11, 29(1968), ibid, Platinum Metal Reviews, 11, 126(1967).

8. C. C. Sartain, W. D. Ryden and A. W. Lawson, J. Non-Cryst. Solids, 5, 55(1970).

9. H. C. Angus and P. E. Gainsbury, Elec. Comp., 84(1968).

10. F. A. Cotton and J. T. Mague, Inorg. Chem., 5, 317(1966).

11. J. M. Fletcher, W. E. Gardner, B. F. Greenfield, M. J. Holdoway, and M. H. Rand, J. Chem. Soc. (A) p. 653(1968).

12. D. B. Rogers, R. D. Shannon, A. W. Sleight, and J. L. Gillson, Inorg. Chem., 8, 841(1969).

13. K. V. K. Rao and L. Iyengar, Acta. Cryst., A25, 302(1969).

14. C. Boman, Acta. Chem. Scand., 24, 116(1970).

15. W. E. Bell and M. Tagami, J. Phys. Chem., 67, 2432(1963).

16. S. Schukarev and A. Ryabov, Russ. J. Inorg. Chem., 5, 941(1960).

17. H. Schafer, G. Schneidereit, and W. Gehardt, Z. Anorg. allgem. Chem., 319, 327(1963).

18. S. Pizzini and L. Rossi, J. Electrochem. Soc., 117, 244C(1970)(Abstract) Presented at Fall 1970 Meeting of the Electrochem. Soc., 1970.

19. W. Latimer, J. Am. Chem. Soc., 73, 1480(1951).

20. D. Chatterji and R. W. Vest, J. Am. Cer. Soc., to be published Feb. 1971.

21. W. D. Ryden, A. W. Lawson, and C. C. Sartain, Phys. Lett., 26A, 209(1968) ibid, Phys. Rev., 131, 1494(1970)
W. D. Ryden, Ph.D. Thesis, U. of Calif. (1970).

22. S. M. Marcus and S. R. Butler, Phys. Lett., 26A, 518(1968).

23. B. C. Passenheim and D. C. McCollum, J. Chem. Phys., 51, 320(1969).

24. C. Osburn, EE 696 Reports, Sch. of Elec. Eng., Purdue University, Jan. 1968, May 1968.

25. R. T. Slivaka and D. M. Langenberg, Phys. Lett., 28A, 169(1968).

26. J. Mukerji and S. R. Biswas , Glass and Cer. Bull., 14, 30(1967).

27. K. K. Dhar Gupta and J. Mukerji, Trans. Ind. Cer. Soc., 27, 123(1968).

28. J. Mukerji and S. R. Biswas , Trans. Ind. Cer. Soc., 28, 59(1969).